European Journal of Pharmaceutical Sciences 209 (2025) 107107

Contents lists available at ScienceDirect

European Journal of Pharmaceutical Sciences

journal homepage: www.elsevier.com/locate/ejps

Synthesis of 3′-modified xylofuranosyl nucleosides bearing 5′-silyl or -butyryl groups and their antiviral effect against RNA viruses

Miklós Bege [a,†], Krisztina Leiner [b,c,†], Miklós Lovas [a], Réka Pető [a], Ilona Bereczki [a,b], Jan Hodek [d], Jan Weber [d], Anett Kuczmog [b,c], Anikó Borbás [a,b,*]

[a] Department of Pharmaceutical Chemistry, Faculty of Pharmacy, University of Debrecen, Egyetem tér 1, Debrecen 4032, Hungary
[b] National Laboratory of Virology, Szentágothai Research Centre, University of Pécs, Ifjúság útja 20, Pecs 7624, Hungary
[c] Institute of Biology, Faculty of Sciences, University of Pécs, Ifjúság útja 6, Pécs 7624, Hungary
[d] Institute of Organic Chemistry and Biochemistry of the Czech Academy of Sciences, Flemingovo náměstí 2, 16610 Prague 6, Czech Republic

ARTICLE INFO

Keywords:
Severe acute respiratory syndrome coronavirus (SARS-CoV-2)
Chikungunya virus (CHIKV)
Sindbis virus (SINV)
Nucleoside analogue antivirals
Photochemical thiol-ene reaction

ABSTRACT

D-xylofuranosyl nucleoside analogues bearing alkylthio and glucosylthio substituents at the C3′-position were prepared by photoinitiated radical-mediated hydrothiolation reactions from the corresponding 2′,5′-di-O-silyl-3′-exomethylene uridine. Sequential desilylation and 5′-O-butyrylation of the 3′-thiosubstituted molecules produced a 24-membered nucleoside series with diverse substitution patterns, and the compounds were evaluated for their in vitro antiviral activity against three dangerous human RNA viruses, SARS-CoV-2, SINV and CHIKV. Eight compounds exhibited SARS-CoV-2 activity with low micromolar EC_{50} values in Vero E6 cells, and two of them also inhibited virus growth in human Calu cells. The best anti-SARS-CoV-2 activity was exhibited by 2′,5′-di-O-silylated 3′-C-alkylthio nucleosides. Twelve compounds showed in vitro antiviral activity against CHIKV and fourteen against SINV with low micromolar EC_{50} values, with the 5′-butyryl-2′-silyl-3′-alkylthio substitution pattern being the most favorable against both viruses. In the case of the tested nucleosides, removal of the 2′-O-silyl group completely abolished the antiviral activity of the compounds against all three viruses. Overall, the most potent antiviral agent was the disilylated 3′-glucosylthio xylonucleoside, which showed excellent and specific antiviral activity against SINV with an EC_{50} value of 3 μM and no toxic effect at the highest tested concentration of 120 μM.

1. Introduction

The COVID-19 pandemic, caused by the zoonotic coronavirus SARS-CoV-2 (severe acute respiratory syndrome coronavirus 2), has resulted in >770 million reported cases and ~7 million deaths by early 2025. SARS-CoV-2 is a positive-sense, single-stranded, enveloped RNA virus belonging to the genus *Betacoronavirus* of the *Coronaviridae* family. Multiple vaccines have been developed to prevent SARS-CoV-2 infection, but the risk of severe disease remains due to the emergence of new SARS-CoV-2 variants (Thakur et al., 2022). In addition to vaccines, some small molecule antiviral agents have been approved for the treatment of SARS-CoV-2 infection. These include nucleoside analogues (Fig. 1A) that target the viral RNA-dependent RNA polymerase, such as remdesivir (Gordon et al. 2020) and molnupiravir (Bernal et al. 2021; Syed, 2022) as well as the combination drug Paxlovid (nimratrelvir in combination with ritonavir as a pharmacokinetic enhancer) that inhibits the main viral protease (Owen et al. 2021). Despite the promising efficacy of these drugs, their widespread use has limitations. Remdesivir requires intravenous administration, molnupiravir has a mutagenic mechanism of action (Sanderson et al. 2023) and Paxlovid is contraindicated in many patients due to harmful drug-drug interactions (Bege and Borbás 2024). These disadvantages indicate that continued research is needed to identify novel oral drug candidates, and the emergence of new SARS-CoV-2 mutants highlights the need for more potent and broad-spectrum antiviral drugs.

In the search for novel oral treatments for COVID-19, several derivatives of the parent nucleoside of remdesivir, including **VV116** and **GS-5245**, have been identified as oral drug candidates (Fig. 1B). The oral availability and broad-spectrum antiviral efficacy of the 5′-isobutyrate derivative **GS-5245** (Obeldesivir) against single-stranded RNA

* Corresponding author.
E-mail addresses: borbas.aniko@pharm.unideb.hu, borbas.aniko@science.unideb.hu (A. Borbás).
† These authors contributed equally to this work.

https://doi.org/10.1016/j.ejps.2025.107107
Received 22 January 2025; Received in revised form 18 April 2025; Accepted 21 April 2025
Available online 21 April 2025

viruses have recently been demonstrated and this compound is currently undergoing phase 3 trials for the treatment of COVID-19 (Mackman et al., 2023). **VV116**, a deuterated and per-*O*-isobutyrated prodrug, has been approved in China for the treatment of mild to moderate COVID-19 patients (Cao et al. 2022). In this context, it is worth mentioning celgosivir, a non-nucleoside antiviral compound that also contains a butyric acid ester group (Anderson et al. 1990). Celgosivir, an oral prodrug of the natural iminosugar castanospermine, has been shown to be a potent antiviral drug candidate against several viruses, including HCV, HIV-1, DENV, and SARS-CoV-2 (Rajasekharan et al. 2021; Clarke et al. 2021.).

Recently, our research group demonstrated that the photoinitiated thiol-ene coupling reaction (also known as thio-click reaction) can be used to efficiently prepare novel nucleoside analogues bearing diverse thio substituents on the furanose ring (Bege et al. 2017). The radical mediated thiol-ene addition reaction proceeded with complete regio and high stereoselectivity on the furanosyl exomethylene derivatives of nucleosides, affording 2′-thiosubstituted D-arabino-, 3′-thiosubstituted D-xylo- and 5′-thiosubstituted L-lyxo-nucleosides in good to excellent yields. The nucleoside analogues obtained exhibited antimalarial, (Bege et al. 2023) antitumor, (Bege et al. 2019; Kiss et al. 2021) or antiviral activity (Bege et al. 2022) depending on the type of thio substituent and the site of modification. Most of the 3-substituted xylonucleosides produced showed significant cytotoxicity, (Bege et al. 2019) but some uridine derivative also showed promising antiviral activity against human coronavirus HCoV-229E and SARS-CoV-2 below toxic concentrations (Fig. 1C). As a continuation of our research, we planned to prepare a series of novel 3′-substituted uridine analogs using different thiols and convert them into 5′-butyryl derivatives, as the 5′-butyric acid ester is an important structural element in broad-spectrum antiviral agents (the butyrate ester motif is highlighted in blue in Fig. 1). Here, we present the synthesis of novel xylofuranosyl nucleosides based on thio-click chemistry (Fig. 1D) and evaluate their antiviral activity against three RNA viruses, including SARS-CoV-2, Chikungunya virus (CHIKV), and Sindbis virus (SINV). CHIKV and SINV are emerging arthropod-borne viruses (transmitted by mosquitos) with positive single-stranded RNA genomes

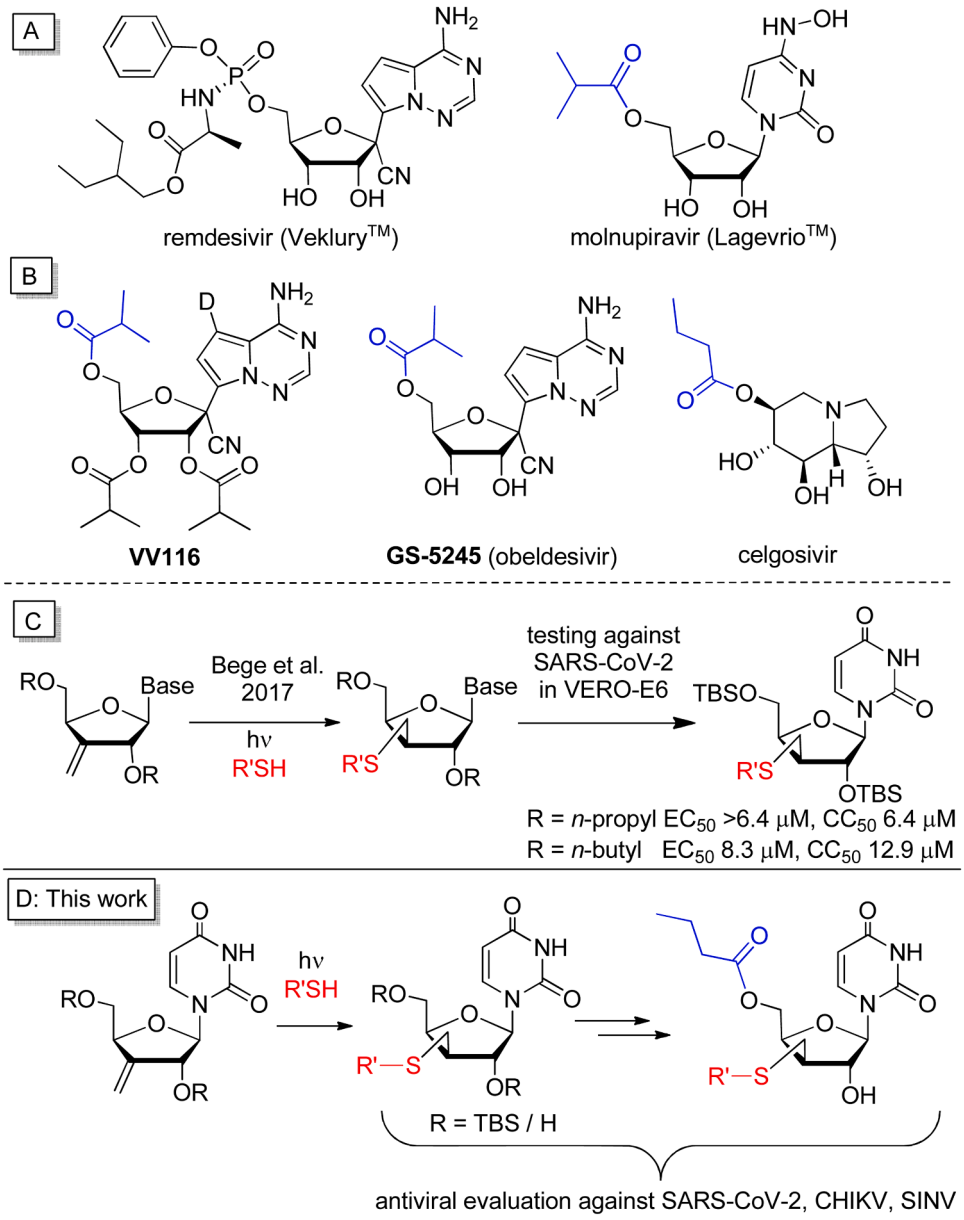

Fig. 1. A: Nucleoside analog drugs for the treatment of COVID-19; B: Clinical antiviral candidates with broad-spectrum activity against RNA viruses; C: Synthesis of 3′-thiosubstituted xylonucleosides and preliminary anti-SARS-CoV-2 activity data; D: This work. (TBS: *tert*-butyldimethylsilyl).

similar to SARS-CoV-2, causing acute febrile illness and long-term joint pain. (Vu et al. 2017; Laine et al. 2004). CHIKV has caused explosive epidemics in Africa over the past 20 years, and has rapidly spread to Asia and to the Americas (Weaver and Lecuit 2015), while SINV mainly causes disease in Southern Africa and Northern Europe. There are currently no specific drugs available to treat CHIKV and SINV infections (Adouchief et al. 2016; Weaver et al. 2018), and the development of effective antivirals against these pathogens is urgently needed.

2. Materials and metods

2.1. Chemistry

2.1.1. General methods

Compounds **1, 2f, 4** and **8** were prepared according to literature procedures. (Bege et al. 2017; Bege et al. 2019; Jana and Misra 2013) 2, 2-Dimethoxy-2-phenylacetophenone (DPAP), ethyl-, *n*-butyl-, *i*-propyl-, *tert*-butyl- and *n*-hexyl-mercaptans were purchased from Sigma-Aldrich Chemical Co. and used without further purification. Optical rotations were measured at room temperature with a Perkin-Elmer 241 automatic polarimeter. TLC was performed on Kieselgel 60 F254 (Merck) with detection by UV-light (254 nm) and immersing into sulfuric acidic ammon ium molybdate solution or 5 % ethanolic sulfuric acid followed by heating. Flash column chromatography was performed on silica gel 60 (Merck, 0.040–0.063 mm). Organic solutions were dried over anhydrous Na2SO4 and concentrated in vacuum. The ^{1}H NMR (360 and 400 MHz) and ^{13}C NMR (90 and 100 MHz) spectra were recorded with Bruker DRX-360 and Bruker DRX-400 spectrometers at 25 °C. Chemical shifts are referenced to Me_4Si (0.00 ppm for ^{1}H) and to the residual solvent signals ($CDCl_3$: 77.2, DMSO-d_6: 39.5, CD_3OD: 49.0 for ^{13}C). Two-dimensional COSY and ^{1}H−^{13}C HSQC experiments were used to assist NMR assignments. MALDI-TOF MS analyses of the compounds were carried out in the positive reflectron mode using a Bruker Autoflex Speed mass spectrometer equipped with a time-of-flight (TOF) mass analyzer. 2,5-Dihydroxybenzoic acid (DHB) was used as matrix and $F_3CCOONa$ as cationising agent in DMF. The photoinitiated reactions were carried out in a borosilicate vessel by irradiation with a low-pressure Hg-lamp giving maximum emission at 365 nm, without any caution to exclude air or moisture.

2.1.2. Synthesis of the new compounds

1-[3′-Deoxy-3′-C-(ethylsulfanylmethyl)-2′,5′-di-*O*-(*tert*-butyldimethylsilyl)-β-D-xylofuranosyl]-uracil (3)

1 (234 mg, 0.5 mmol) was dissolved in toluene (2 mL) and EtSH (288 μL, 4.0 mmol, 8.0 equiv.) and DPAP (12.8 mg, 0.05 mmol, 0.1 equiv.) were added and cooled to −80 °C. The reaction mixture was irradiated at −80 °C for 4 × 15 min. The solvent was evaporated under reduced pressure and the crude product was purified by flash chromatography (hexane/acetone 9/1) to give **3** (208 mg, 78 %, D-xylo:D-ribo ratio = 12:1) as a colorless syrup. $[\alpha]_D$ = +75.7 (*c* = 0.14, $CHCl_3$), Rf = 0.34 (CH_2Cl_2/acetone 95/5), ^{1}H NMR (360 MHz, $CDCl_3$) *δ* (ppm) 7.96 (d, *J* = 8.1 Hz, 1H, H-6), 5.92 (d, *J* = 6.7 Hz, 1H, H-1′), 5.68 (d, *J* = 8.0 Hz, 1H, H-5), 4.28 (d, *J* = 7.4 Hz, 1H, H-4′), 4.14 – 4.06 (m, 1H, H-2′), 3.95 (d, *J* = 11.7 Hz, 1H, H-5′a), 3.85 (dd, *J* = 11.8, 1.9 Hz, 1H, H-5′b), 2.78 – 2.65 (m, 3H, H-3′, S*CH*$_2$), 2.54 (q, *J* = 7.4 Hz, 2H, CH_3CH_2), 1.24 (t, *J* = 7.3 Hz, 3H, CH_3CH_2), 0.92 (s, 9H, *t*-Bu), 0.83 (s, 9H, *t*-Bu), 0.11 (s, 6H, 2 x Si*CH*$_3$), −0.03 (s, 3H, Si*CH*$_3$), −0.14 (s, 3H, Si*CH*$_3$). ^{13}C NMR (90 MHz, $CDCl_3$) *δ* (ppm) 163.0, 150.7 (2C, C-2, C-4), 140.7 (1C, C-6), 102.9 (1C, C-5), 87.8 (1C, C-1′), 79.5, 77.4 (2C, C-2′, C-4′), 63.7 (1C, C-5′), 46.7 (1C, C-3′), 28.4, 26.2 (2C, 2 x S*CH*$_2$), 26.1, 25.6 (6C, 2 x Si*C*(*CH*$_3$)$_3$), 14.7 (1C, *CH*$_3$CH$_2$), −4.5, −4.6, −5.3, −5.6 (4C, *4* x Si*CH*$_3$). MALDI-TOF MS: m/z calcd for $C_{24}H_{46}N_2NaO_5SSi_2$ [*M*+Na]$^{+}$ 553.2558 found 553.2557.

1-[3′-Deoxy-3′-C-(ethylsulfanylmethyl)-2′-*O*-(*tert*-butyldimethylsilyl)-β-D-xylofuranosyl]-uracil (9)

3 (174 mg, 0.33 mmol) was dissolved in THF (3 mL) and cooled to 0 °C. Then, the mixture of TFA (2 mL) and H_2O (2 mL) was added and stirred vigorously at 0 °C for 2 h. The reaction mixture was diluted with sat. aq. $NaHCO_3$ (100 mL) and extracted with CH_2Cl_2 (3 × 50 mL). The organic phase was dried over Na_2SO_4, filtered and concentrated under reduced pressure. The residue was purified by flash chromatography (CH_2Cl_2/acetone 9/1) to give **9** (108 mg, 80 %) as a white solid. $[\alpha]_D$ = +40.0 (*c* = 0.14, $CHCl_3$), Rf = 0.28 (CH_2Cl_2/acetone 9/1), ^{1}H NMR (360 MHz, $CDCl_3$) *δ* (ppm) 8.79 (s, 1H, N*H*), 7.59 (d, *J* = 8.0 Hz, 1H, H-6), 5.74 (d, *J* = 7.9 Hz, 1H, H-5), 5.41 (d, *J* = 6.5 Hz, 1H, H-1′), 4.57 – 4.44 (m, 1H, H-2′), 4.34 (d, *J* = 8.4 Hz, 1H, H-4′), 3.88 (s, 2H, H-5′ab), 3.12 (s, 1H, O*H*), 2.80 (dt, *J* = 12.8, 10.7 Hz, 2H, SC*H*$_2$), 2.65 – 2.50 (m, 3H, SC*H*$_2$, H-3′), 0.83 (s, 9H, *t*-Bu), 0.02, −0.12 (2 x s, 2 × 3H, 2 x Si*CH*$_3$). ^{13}C NMR (90 MHz, $CDCl_3$) δ (ppm) 142.9 (1C, C-6), 102.9 (1C, C-5), 93.5 (1C, C-1′), 80.1, 75.5 (2C, C-2′, C-4′), 62.4 (1C, C-5′), 46.8 (1C, C-3′), 28.7, 26.3 (2C, 2 x S*C*H$_2$), 25.7 (3C, Si*C*(*C*H$_3$)$_3$), 14.7 (1C, *C*H$_3$CH$_2$), −4.4, −4.7 (2C, *2* x Si*C*H$_3$). MALDI-TOF MS: m/z calcd for $C_{18}H_{32}N_2NaO_5SSi$ [*M*+Na]$^{+}$ 439.1693 found 439.1692.

1-[3′-Deoxy-3′-C-(ethylsulfanylmethyl)-5′-*n*-butyryl-2′-*O*-(*tert*-butyldimethylsilyl)-β-D-xylofuranosyl]-uracil (15)

9 (78 mg, 0.19 mmol) was dissolved in dry pyridine (1 mL) and butyryl chloride (23 μL, 0.22 mmol, 1.2 equiv.) was added and stirred overnight. The reaction mixture was diluted with CH_2Cl_2 (10 0 mL) and extracted with 10 % aq. $NaHSO_4$ (3 × 50 mL) and brine (1 × 50 mL). The organic phase was dried over Na_2SO_4, filtered and concentrated under educed pressure. The residue was purified by flash chromatography (CH_2Cl_2/acetone 95/5 →9/1) to give **15** (73 mg, 79 %) as a colorless syrup. $[\alpha]_D$ = +59.4 (*c* = 0.18, $CHCl_3$), Rf = 0.48 (CH_2Cl_2/acetone 9/1), ^{1}H NMR (360 MHz, $CDCl_3$) *δ* (ppm) 9.65 (s, 1H, N*H*), 7.54 (d, *J* = 8.0 Hz, 1H, H-6), 5.73 (s, 2H, H-1′, H-5), 4.55 (s, 1H, H-4′), 4.44 (dd, *J* = 10.4, 6.4 Hz, 1H, H-5′a), 4.26 (d, *J* = 8.6 Hz, 2H, H-5′a, H-2′), 2.62 – 2.41 (m, 5H, H-3′, 2 x S*CH*$_2$), 2.32 (t, *J* = 7.0 Hz, 2H, $CH_3CH_2CH_2CO$), 2.00 (d, *J* = 5.6 Hz, 1H), 1.66 (dd, *J* = 14.1, 6.8 Hz, 2H, $CH_3CH_2CH_2CO$), 1.39–1.30 (m, 3H, *CH*$_3$CH$_2$) 0.97 – 0.92 (m, 3H, *CH*$_3$CH$_2$CH$_2$CO), 0.84 (s, 9H, *t*-Bu), 0.04, −0.01 (2 x s, 2 × 3H, 2 x Si*CH*$_3$). ^{13}C NMR (90 MHz, $CDCl_3$) *δ* (ppm) 173.0 (1C, $CH_3CH_2CH_2CO$), 163.4, 150.5 (2C, C-2, C-4), 139.5 (1C, C-6), 102.7 (1C, C-5), 90.8 (1C, C-1′), 78.2, 77.9 (2C, C-2′, C-4′), 63.5 (1C, C-5′), 47.2 (1C, C-3′), 36.3 (1C, $CH_3CH_2CH_2CO$), 29.8, 28.6, 26.4 (3C, 3 x *C*H$_2$), 25.6 (3C, Si*C*(*CH*$_3$)$_3$), 18.5 (2C, $CH_3CH_2CH_2CO$, *t*-Bu C_q), 14.6 (1C, *CH*$_3$CH$_2$), 13.8 (1C, *CH*$_3$CH$_2$CH$_2$CO), −4.6, −4.7 (2C, *2* x Si*CH*$_3$). MALDI-TOF MS: m/z calcd for $C_{22}H_{38}N_2NaO_6SSi$ [*M*+Na]$^{+}$ 509.2112 found 509.2110.

1-[3′-Deoxy-3′-C-(ethylsulfanylmethyl)-5′-*n*-butyryl-β-D-xylofuranosyl]-uracil (21)

15 (54 mg, 0.1 1 mmol) was dissolved in 90 % TFA (1 mL) and stirred for 4 h. The reaction mixture was diluted with sat. aq. $NaHCO_3$ (100 mL) and extracted with CH_2Cl_2 (3 × 50 mL). The organic phase was dried over Na_2SO_4, filtered and concentrated under reduced pressure. The crude product was purified by flash chromatography (EtOAc/MeOH 99/1) to give **21** (25 mg, 60 %) as a colorless syrup. $[\alpha]_D$ = +77.0 (*c* = 0.10, $CHCl_3$), Rf = 0.6 (EtOAc/MeOH 95/5), ^{1}H NMR (360 MHz, $CDCl_3$) *δ* (ppm) 9.76 (s, 1H, N*H*), 7.59 (d, *J* = 8.2 Hz, 1H, H-6), 5.70 (d, *J* = 8.2 Hz, 1H, H-5), 5.58 (d, *J* = 4.8 Hz, 1H, H-1′), 4.65 (dt, *J* = 7.3, 3.5 Hz, 1H, H-4′), 4.36 – 4.24 (m, 3H, H-5′ab, OH), 4.14 (dd, *J* = 8.3, 4.8 Hz, 1H, H-2′), 2.88 – 2.75 (m, 3H, H-3′, 3′-SC*H*$_2$), 2.56 (dd, *J* = 14.8, 7.4 Hz, 2H, CH_3CH_2), 2.26 – 2.16 (m, 2H, $CH_3CH_2CH_2CO$), 1.60 (dd, *J* = 14.8, 7.4 Hz, 2H, $CH_3CH_2CH_2CO$), 1.25 (d, *J* = 7.4 Hz, 3H, *CH*$_3$CH$_2$), 0.91 (t, *J* = 7.4 Hz, 3H, *CH*$_3$CH$_2$CH$_2$CO). ^{13}C NMR (90 MHz, $CDCl_3$) *δ* (ppm) 173.1 (1C, $CH_3CH_2CH_2CO$), 152.4 (1C, uracil *C*O), 139.5 (1C, C-6), 101.9 (1C, C-5), 93.7 (1C, C-1′), 80.3, 79.9 (2C, C-2′, C-4′), 63.5 (1C, C-5′), 46.8 (1C, C-3′), 36.3 (1C, $CH_3CH_2CH_2CO$), 29.1, 26.6 (2C, 2 x S*CH*$_2$), 18.4 (1C, $CH_3CH_2CH_2CO$), 14.7 (1C, *CH*$_3$CH$_2$), 13.8 (1C, *CH*$_3$CH$_2$CH$_2$CO). MALDI-TOF MS: m/z calcd for $C_{16}H_{24}N_2NaO_6S$ [*M*+Na]$^{+}$ 395.1247 found 395.1244.

1-[3′-Deoxy-3′-C-(butylsulfanylmethyl)-2′-*O*-(*tert*-butyldimethylsilyl)-β-D-xylofuranosyl]-uracil (10)

4 (166 mg, 0.29 mmol) was dissolved in THF (3 mL) and cooled to 0 °C. Then, the mixture of TFA (2 mL) and H_2O (2 mL) was added and

stirred vigorously at 0 °C for 2 h. The reaction mixture was diluted with sat. aq. $NaHCO_3$ (100 mL) and extracted with CH_2Cl_2 (3 × 50 mL). The organic phase was dried over Na_2SO_4, filtered and concentrated under reduced pressure. The residue was purified by flash chromatography (CH_2Cl_2/acetone 9/1) to give **10** (89 mg, 68 %) as a colorless syrup. [α]$_D$= +61.8 (c = 0.11, $CHCl_3$), Rf = 0.12 (CH_2Cl_2/aceton 9/1), ^{1}H NMR (360 MHz, $CDCl_3$) δ (ppm) 8.75 (s, 1H, N*H*), 7.59 (d, J = 8.1 Hz, 1H, H-6), 5.74 (dd, J = 8.0, 2.1 Hz, 1H, H-5), 5.41 (d, J = 6.6 Hz, 1H, H-1′), 4.48 (dd, J = 9.0, 6.7 Hz, 1H, H-2′), 4.34 (d, J = 8.4 Hz, 1H, H-4′), 3.96 – 3.83 (m, 2H, H-5′ab), 3.09 (dd, J = 6.3, 2.9 Hz, 1H, O*H*), 2.89 – 2.78 (m, 1H, 3′-SC*H*$_2$a), 2.73 (dd, J = 12.8, 3.9 Hz, 1H, 3′-SC*H*$_2$b), 2.60 (ddd, J = 14.6, 7.8, 3.7 Hz, 1H, H-3′), 2.51 (t, J = 7.3 Hz, 2H, $CH_3CH_2CH_2CH_2$), 1.54 (ddd, J = 10.1, 7.4, 3.2 Hz, 2H, $CH_3CH_2CH_2CH_2$), 1.37 (dt, J = 14.7, 7.4 Hz, 2H, $CH_3CH_2CH_2CH_2$), 0.89 (t, J = 7.3 Hz, 3H, $CH_3CH_2CH_2CH_2$), 0.83 (s, 9H, *t*-Bu), 0.02, −0.12 (2 x s, 2 × 3H, 2 x SiCH_3). ^{13}C NMR (90 MHz, $CDCl_3$) δ (ppm) 142.8 (1C, C-6), 102.9 (1C, C-5), 93.4 (1C, C-1′), 80.0, 75.5 (2C, C-2′, C-4′), 62.3 (1C, C-5′), 46.8 (1C, C-3′), 32.1 (1C, $CH_3CH_2CH_2CH_2$), 28.9 (1C, 3′-SCH_2), 31.6, 21.9 (2C, $CH_3CH_2CH_2CH_2$, $CH_3CH_2CH_2CH_2$), 25.6 (3C, SiC(CH_3)$_3$), 13.7 (1C, $CH_3CH_2CH_2CH_2$), −4.5, −4.7 (2C, *2* x SiCH_3). MALDI-TOF MS: m/z calcd for $C_{20}H_{36}N_2NaO_5SSi$ [M+Na]$^+$ 467.2006, found 467.2019.

1-[3′-Deoxy-3′-C-(butylsulfanylmethyl)-5′-*n*-butyryl-2′-*O*-(*tert*-butyldimethylsilyl)-β-D-xylofuranosyl]-uracil (16)

10 (68 mg, 0.15 mmol) was dissolved in dry pyridine (1 mL) and butyryl chloride (19 μL, 0.18 mmol, 1.2 equiv.) was added and stirred overnight. The reaction mixture was diluted with CH_2Cl_2 (10 0 mL) and extracted with 10 % aq. $NaHSO_4$ (3 × 50 mL) and brine (1 × 50 mL). The organic phase was dried over Na_2SO_4, filtered and concentrated under educed pressure. The residue was purified by flash chromatography (CH_2Cl_2/acetone 95/5 →9/1) to give **16** (56 mg, 72 %) as a colorless syrup. [α]$_D$ = +66.0 (c = 0.10, $CHCl_3$), Rf = 0.36 (CH_2Cl_2/aceton 95/5), ^{1}H NMR (360 MHz, $CDCl_3$) δ (ppm) 9.77 (s, 1H, N*H*), 7.53 (d, J = 8.1 Hz, 1H, H-6), 5.74 (d, J = 8.3 Hz, 1H, H-5), 5.71 (d, J = 4.5 Hz, 1H, H-1′), 4.57 – 4.51 (m, 1H, H-4′), 4.43 (dd, J = 12.2, 5.7 Hz, 1H, H-5′a), 4.29 – 4.20 (m, 2H,H-2′, H-5′b), 2.44 (dt, J = 8.5, 5.4 Hz, 5H, H-3′, 2 x SCH_2), 2.30 (dd, J = 15.1, 7.6 Hz, 2H, $CH_3CH_2CH_2CO$), 1.65 (dq, J = 14.1, 7.1 Hz, 2H, $CH_3CH_2CH_2CO$), 1.54 – 1.43 (m, 2H, $CH_3CH_2CH_2CH_2$), 1.34 (td, J = 14.4, 7.1 Hz, 2H, $CH_3CH_2CH_2CH_2$), 0.93 (t, J = 7.4 Hz, 3H, CH_3), 0.89 – 0.86 (m, 3H, CH_3), 0.83 (s, 9H, *t*-Bu), 0.03, −0.02 (2 x s, 2 × 3H, 2 x SiCH_3). ^{13}C NMR (90 MHz, $CDCl_3$) δ (ppm) 173.1 (1C, $CH_3CH_2CH_2CO$), 163.5, 150.6 (2C, C-2, C-4), 139.6 (1C, C-6), 102.7 (1C, C-5), 90.8 (1C, C-1′), 78.2, 78.0 (2C, C-2′, C-4′), 63.5 (1C, C-5′), 47.3 (1C, C-3′), 36.3 (1C, $CH_3CH_2CH_2CO$), 32.3 (1C, $CH_3CH_2CH_2CH_2$), 29.0 (1C, 3′-SCH_2), 31.5, 21.9 (2C, $CH_3CH_2CH_2CH_2$, $CH_3CH_2CH_2CH_2$), 25.6 (3C, SiC(CH_3)$_3$), 18.5 (2C, $CH_3CH_2CH_2CO$, *t*-Bu C_q), 13.8, 13.7 (2C, $CH_3CH_2CH_2CH_2$, $CH_3CH_2CH_2CO$), −4.6, −4.7 (2C, *2* x SiCH_3). MALDI-TOF MS: m/z calcd for $C_{24}H_{42}N_2NaO_6SSi$ [M+Na]$^+$ 537.2425, found 537.2429.

1-[3′-Deoxy-3′-C-(butylsulfanylmethyl)-5′-*n*-butyryl-2′-*O*-(*tert*-butyldimethylsilyl)-β-D-xylofuranosyl]-uracil (22)

16 (35 mg, 0.06 7 mmol) was dissolved in 90 % aq. TFA and stirred for 8 h at r.t. The reaction mixture was diluted with sat. aq. $NaHCO_3$ (50 mL) and extracted with CH_2Cl_2 (3 × 50 mL). The organic phase was dried over Na_2SO_4, filtered and evaporated under reduced pressure. The residue was purified by flash chromatography (CH_2Cl_2/acetone 9/1) to give **22** (25 mg, 93 %) as a colorless syrup. [α]$_D$ = +71.8 (c = 0.28, $CHCl_3$), Rf = 0.21 (CH_2Cl_2/acetone 9/1), ^{1}H NMR (360 MHz, $CDCl_3$) δ (pm) 10.13 (s, 1H, N*H*), 7.63 (d, J = 8.2 Hz, 1H, H-6), 5.73 (d, J = 8.2 Hz, 1H, H-5), 5.65 (d, J = 4.8 Hz, 1H, H-1′), 4.67 (dt, J = 7.3, 3.6 Hz, 1H, H-4′), 4.56 (s, 1H, O*H*), 4.41 – 4.28 (m, 2H, H-5′ab), 4.18 (dd, J = 6.8, 5.3 Hz, 1H, H-2′), 2.82 (dq, J = 8.1, 5.7 Hz, 2H), 2.61 – 2.52 (m, 2H), 2.51 – 2.44 (m, 1H), 2.33 – 2.17 (m, 2H, $CH_3CH_2CH_2CO$), 1.69 – 1.52 (m, 4H, $CH_3CH_2CH_2CO$), 1.40 (td, J = 14.6, 7.3 Hz, 2H, $CH_3CH_2CH_2CH_2$), 1.25 (s, 2H, $CH_3CH_2CH_2CH_2$), 0.97 – 0.85 (m, 6H, 2 x CH_3). ^{13}C NMR (90 MHz, $CDCl_3$) δ (ppm) 172.9 (1C, $CH_3CH_2CH_2CO$), 163.7, 151.9 (2C, C-2, C-4), 139.5 (1C, C-6), 102.0 (1C, C-4), 93.4 (1C, C-1′), 80.1, 79.7 (2C, C-2′, C-4′), 63.5 (1C, C-5′), 46.8 (1C, C-3′), 36.3 (1C, $CH_3CH_2CH_2CO$), 32.4 (1C, $CH_3CH_2CH_2CH_2$), 31.6, 29.6 (2C, 3′-SCH_2, $CH_3CH_2CH_2CH_2$), 22.0 (1C, $CH_3CH_2CH_2CH_2$), 18.4 (1C, $CH_3CH_2CH_2CO$), 13.8 (2*C*, 2 x *C*H$_3$). MALDI-TOF MS: m/z calcd for $C_{18}H_{28}N_2NaO_6S$ [M+Na]$^+$ 423.1560, found 423.1552.

1-[3′-Deoxy-3′-C-(*n*-hexyl-sulfanylmethyl)-2′,5′-di-*O*-(*tert*-butyldimethylsilyl)-β-D-xylofuranosyl]-uracil (5)

1 (234 mg, 0.5 mmol) was dissolved in toluene (2 mL) and HexSH (567 μL, 4.0 mmol, 8.0 equiv.) and DPAP (12.8 mg, 0.05 mmol, 0.1 equiv.) were added and cooled to −40 °C. The reaction mixture was irradiated at −40 °C for 3 × 15 min. The solvent was evaporated under reduced pressure and the crude product was purified by flash chromatography (hexane/acetone 9/1) to give **5** (231 mg, 79 %, D-xylo:D-ribo ratio = 13.5:1) as a colorless syrup. [α]$_D$ = +67.6 (c = 0.21, $CHCl_3$), Rf = 0.44 (hexane/acetone 9/1), ^{1}H NMR (360 MHz, $CDCl_3$) δ (ppm) 8.42 (s, 1H, N*H*), 7.97 (d, J = 8.2 Hz, 1H, H-6), 5.92 (d, J = 6.7 Hz, 1H, H-1′), 5.68 (dd, J = 8.1, 2.3 Hz, 1H, H-5), 4.28 (d, J = 7.1 Hz, 1H, H-4′), 4.09 (dd, J = 8.5, 7.0 Hz, 1H, H-2′), 3.99 – 3.91 (m, 1H, H-5′a), 3.85 (dd, J = 11.8, 2.2 Hz, 1H, H-5′b), 2.76 – 2.64 (m, 4H, SCH_2, H-3′), 2.53 – 2.47 (m, 2H), 1.62 – 1.48 (m, 4H), 1.36 (dt, J = 10.4, 5.1 Hz, 2H), 1.30 – 1.20 (m, 6H), 0.93, 0.83 (2 x s, 2 × 9H, 2 x *t*-Bu), 0.12 (s, 6H, 2 x SiCH_3), −0.03 (s, 3H, SiCH_3), −0.14 (s, 3H, SiCH_3). ^{13}C NMR (90 MHz, $CDCl_3$) δ (ppm) 163.8, 150.6 (2C, C-2, C-4), 140.7 (1C, C-6), 102.8 (1C, C-5), 87.9 (1C, C-1′), 79.5, 77.4 (2C, C-2′, C-4′), 63.7 (1C, C-5′), 46.7 (1C, C-3′), 32.4 (1C, $CH_3CH_2CH_2CH_2CH_2CH_2$), 31.6 (1C, $CH_3CH_2CH_2CH_2CH_2CH_2$), 29.6 (1C, $CH_3CH_2CH_2CH_2CH_2CH_2$), 28.9 (1C, $CH_3CH_2CH_2CH_2CH_2CH_2$), 28.6 (1C, 3′-SCH_2), 22.7 (1C, $CH_3CH_2CH_2CH_2CH_2CH_2$), 26.1, 25.7 (6C, 2 x SiC(CH_3)$_3$), 17.8 (1C, *t*-Bu C_q), 14.2 (1C, $CH_3CH_2CH_2CH_2CH_2CH_2$), −4.5, −4.6, −5.3, −5.5 (4C, *4* x SiCH_3). MALDI-TOF MS: m/z calcd for $C_{28}H_{54}N_2NaO_5SSi_2$ [M+Na]$^+$ 609.3184, found 609.3177.

1-[3′-Deoxy-3′-C-(*n*-hexyl-sulfanylmethyl)-2′-*O*-(*tert*-butyldimethylsilyl)-β-D-xylofuranosyl]-uracil (11)

5 (205 mg, 0.35 mmol) was dissolved in THF (3 mL) and cooled to 0 °C. Then, the mixture of TFA (2 mL) and H_2O (2 mL) was added and stirred vigorously at 0 °C for 2 h. The reaction mixture was diluted with sat. aq. $NaHCO_3$ (100 mL) and extracted with CH_2Cl_2 (3 × 50 mL). The organic phase was dried over Na_2SO_4, filtered and concentrated under reduced pressure. The residue was purified by flash chromatography (CH_2Cl_2/acetone 9/1) to give **11** (146 mg, 88 %) as a colorless syrup. [α]$_D$ = +42.7 (c = 0.15, $CHCl_3$), Rf = 0.2 (CH_2Cl_2/acetone 9/1), ^{1}H NMR (360 MHz, $CDCl_3$) δ (ppm) 8.72 (s, 1H, N*H*), 7.59 (d, J = 8.1 Hz, 1H, H-6), 5.74 (d, J = 8.0 Hz, 1H, H-5), 5.41 (d, J = 6.6 Hz, 1H, H-1′), 4.47 (dd, J = 9.0, 6.8 Hz, 1H, H-2′), 4.34 (d, J = 8.3 Hz, 1H, H-4′), 3.97 – 3.83 (m, 2H, H-5′ab), 3.07 (s, 1H, O*H*), 2.89 – 2.79 (m, 1H, 3′-SC*H*$_2$a), 2.73 (dd, J = 12.8, 3.9 Hz, 1H, 3′-SC*H*$_2$b), 2.65 – 2.55 (m, 1H, H-3′), 2.50 (t, J = 7.0 Hz, 2H, Hex SCH_2), 1.67 – 1.52 (m, 2H, $CH_3CH_2CH_2CH_2CH_2CH_2$), 1.31–1.38 (m, 2H, $CH_3CH_2CH_2CH_2CH_2CH_2$), 1.30–1.24 (m, 4H, $CH_3CH_2CH_2CH_2CH_2CH_2$ + $CH_3CH_2CH_2CH_2CH_2CH_2$), 0.89–0.84 (m, 3H, Hex CH_3), 0.83 (s, 9H, *t*-Bu), 0.02, −0.12 (2 x s, 2 × 3H, 2 x SiCH_3). ^{13}C NMR (90 MHz, $CDCl_3$) δ (ppm) 142.9 (1C, C-6), 102.9 (1C, C-5), 93.5 (1C, C-1′), 80.1 (1C, C-4′), 75.5 (1C, C-2′), 62.3 (1C, C-5′), 46.7 (1C, C-3′), 32.4 (1C, Hex SCH_2), 31.5 (1C, $CH_3CH_2CH_2CH_2CH_2CH_2$), 29.5 (1C, $CH_3CH_2CH_2CH_2CH_2CH_2$), 29.0 (1C, $CH_3CH_2CH_2CH_2CH_2CH_2$), 22.6 (1C, $CH_3CH_2CH_2CH_2CH_2CH_2$), 25.6 (3C, SiC(CH_3)$_3$), 17.8 (1C, *t*-Bu C_q), −4.7 (2C, *2* x SiCH_3). MALDI-TOF MS: m/z calcd for $C_{22}H_{40}N_2NaO_5SSi$ [M+Na]$^+$ 495.2319, found 495.2329.

1-[3′-Deoxy-3′-C-(hexylsulfanylmethyl)-5′-*n*-butyryl-2′-*O*-(*tert*-butyldimethylsilyl)-β-D-xylofuranosyl]-uracil (17)

11 (110 mg, 0.19 mmol) was dissolved in dry pyridine (1 mL) and butyryl chloride (23 μL, 0.22 mmol, 1.2 equiv.) was added and stirred overnight. The reaction mixture was diluted with CH_2Cl_2 (10 0 mL) and extracted with 10 % aq. $NaHSO_4$ (3 × 50 mL) and brine (1 × 50 mL). The organic phase was dried over Na_2SO_4, filtered and concentrated under reduced pressure. The residue was purified by flash chromatography (CH_2Cl_2/acetone 95/5) to give **17** (60 mg, 58 %) as a colorless syrup. [α]$_D$ = +55.3 (c = 0.15, $CHCl_3$), Rf = 0.8 (CH_2Cl_2/acetone 9/1), ^{1}H NMR

(360 MHz, $CDCl_3$) δ (ppm) 8.53 (s, 1H, N*H*), 7.53 (d, $J = 8.2$ Hz, 1H, H-6), 5.73 (dd, $J = 9.9$, 3.4 Hz, 2H, H-5, H-1′), 4.60 – 4.52 (m, 1H, H-4′), 4.45 (dd, $J = 12.2$, 5.7 Hz, 1H, H-5′a), 4.30 – 4.20 (m, 2H, H-2′, H-5′b), 2.47 (ddd, $J = 16.3$, 10.9, 5.4 Hz, 5H, H-3′, 2 x SCH_2), 2.32 (t, $J = 7.3$ Hz, 2H, COCH_2CH$_2$CH$_3$), 1.75 – 1.62 (m, 2H, COCH$_2$CH_2CH$_3$), 1.51 (dd, $J =$ 14.2, 7.0 Hz, 2H, CH$_3$CH$_2$CH$_2$CH$_2$CH_2CH$_2$), 1.38–1.28 (m, 4H, CH$_3$CH$_2$CH_2CH$_2$CH$_2$CH$_2$ + CH$_3$CH$_2$CH$_2$CH$_2$CH_2CH$_2$CH$_2$), 1.28–1.22 (m, 4H, CH$_3$CH_2CH$_2$CH$_2$CH$_2$CH$_2$), 0.95 (t, $J = 7.4$ Hz, 3H, COCH$_2$CH$_2$CH_3), 0.9–0.84 (m, 12H, *t*-Bu + Hex CH_3), 0.05, −0.01 (2 x s, 2 × 3H, 2 x SiCH_3). ^{13}C NMR (90 MHz, $CDCl_3$) δ (ppm) 139.6 (1C, C-6), 102.7 (1C, C-5), 90.8 (1C, C-1′), 78.3, 78.0 (2C, C-2′, C-4′), 63.6 (1C, C-5′), 47.3 (1C, C-3′), 36.4 (1C, CO*C*H$_2$CH$_2$CH$_3$), 32.7 (1C, CH$_3$CH$_2$CH$_2$*C*H$_2$CH$_2$CH$_2$), 31.5 (1C, CH$_3$CH$_2$*C*H$_2$CH$_2$CH$_2$CH$_2$), 29.5 (1C, CH$_3$CH$_2$CH$_2$*C*H$_2$CH$_2$CH$_2$), 29.1 (1C, CH$_3$CH$_2$CH$_2$CH$_2$*C*H$_2$CH$_2$), 28.6 (1C, 3′-SCH_2), 22.7 (1C, CH$_3$CH$_2$CH$_2$CH$_2$CH$_2$CH$_2$), 25.7 (3C, SiC(*C*H$_3$)$_3$), 18.6 (1C, *t*-Bu C_q), 14.2 (1C, COCH$_2$CH$_2$*C*H$_3$), 13.8 (1C, *C*H$_3$CH$_2$CH$_2$CH$_2$CH$_2$CH$_2$), −4.6, −4.6 (2C, *2* x SiCH_3). MALDI-TOF MS: m/z calcd for $C_{26}H_{46}N_2NaO_6SSi$ $[M+Na]^+$ 565.2738, found 565.2742.

1-[3′-Deoxy-3′-C-(hexylsulfanylmethyl)-5′-*n*-butyryl-β-D-xylofuranosyl]-uracil (23)

17 (40 mg, 0.07 4 mmol) was dissolved in 90 % aq. TFA and stirred for 5 h at r.t. The reaction mixture was diluted with sat. aq. $NaHCO_3$ (50 mL) and extracted with CH_2Cl_2 (3 × 50 mL). The organic phase was dried over Na_2SO_4, filtered and evaporated under reduced pressure. The residue was purified by flash chromatography (CH_2Cl_2/acetone 9/1) to give **23** (26 mg, 85 %) as a colorless syrup. $[\alpha]_D = +94.5$ ($c = 0.11$, $CHCl_3$), Rf = 0.22 (CH_2Cl_2/acetone 9/1), ^{1}H NMR (360 MHz, $CDCl_3$) δ (ppm) 10.05 (s, 1H, N*H*), 7.63 (d, $J = 7.8$ Hz, 1H, H-6), 5.73 (d, $J = 7.9$ Hz, 1H, H-5), 5.64 (s, 1H, H-1′), 4.43 (dd, $J = 117.1$, 57.8 Hz, 6H), 2.82 (s, 2H), 2.53 (dd, $J = 12.6$, 6.5 Hz, 3H), 2.25 (d, $J = 6.4$ Hz, 2H), 1.74 – 1.53 (m, 5H), 1.33 (d, $J = 28.1$ Hz, 7H), 0.93 (dd, $J = 16.6$, 9.5 Hz, 6H). ^{13}C NMR (90 MHz, $CDCl_3$) δ (ppm) 172.8 (1C, CH$_3$CH$_2$CH$_2$*C*O), 163.6, 151.8 (2C, C-2, C-4), 139.5 (1C, C-6), 101.9 (1C, C-5), 93.4 (1C, C-1′), 80.1, 79.7 (2C, C-2′, C-4′), 63.4 (1C, C-5′), 46.8 (1C, C-3′), 36.2 (1C, CH$_3$CH$_2$*C*H$_2$CO), 32.7, 31.4, 29.5, 29.4 (4C, 4 x CH$_2$), 28.5 (1C, CH$_3$CH$_2$*C*H$_2$CH$_2$CH$_2$CH$_2$), 22.6 (1C, CH$_3$*C*H$_2$CH$_2$CH$_2$CH$_2$CH$_2$), 18.3 (1C, CH$_3$*C*H$_2$CH$_2$CO), 14.1, 13.7 (2C, *C*H$_3$CH$_2$CH$_2$CH$_2$CH$_2$CH$_2$, *CH$_3$*CH$_2$CH$_2$CO). MALDI-TOF MS: m/z calcd for $C_{20}H_{32}N_2NaO_6S$ $[M+Na]^+$ 451.1873, found 451.1880.

1-[3′-Deoxy-3′-C-(*i*-propyl-sulfanylmethyl)-2′,5′-di-*O*-(*tert*-butyldimethylsilyl)-β-D-xylofuranosyl]-uracil (6)

1 (234 mg, 0.5 mmol) was dissolved in toluene (2 mL) and *i*-PrSH (371 μL, 4.0 mmol, 8.0 equiv.) and DPAP (12.8 mg, 0.05 mmol, 0.1 equiv.) were added and cooled to 0 °C. The reaction mixture was irradiated at 0 °C for 3 × 15 min. The solvent was evaporated under reduced pressure and the crude product was purified by flash chromatography (hexane/acetone 8/2) to give **6** (236 mg, 87 %, D-xylo:D-ribo ratio = 15:1) as a colorless syrup. $[\alpha]_D = +66.4$ ($c = 0.14$, $CHCl_3$), Rf = 0.6 (hexane/acetone 7/3), ^{1}H NMR (360 MHz, $CDCl_3$) δ (ppm) 8.50 (s, 1H, N*H*), 7.98 (d, $J = 8.2$ Hz, 1H, H-6), 5.92 (d, $J = 6.7$ Hz, 1H, H-1′), 5.69 (dd, $J = 8.1$, 2.1 Hz, 1H, H-5), 4.28 (d, $J = 7.4$ Hz, 1H, H-4′), 4.10 (dd, $J = 8.9$, 6.8 Hz, 1H, H-2′), 3.95 (d, $J = 11.9$ Hz, 1H, H-5′a), 3.85 (dd, $J =$ 11.8, 2.1 Hz, 1H, H-5′b), 2.93 (tt, $J = 13.3$, 6.6 Hz, 1H, SCH_2a), 2.81 – 2.60 (m, 3H, H-3′, SCH_2b, *i*-Pr-CH), 1.25 (dd, $J = 6.6$, 4.7 Hz, 6H, 2 x *i*-Pr CH_3), 0.93 (s, 9H, *t*-Bu), 0.83 (s, 9H, *t*-Bu), 0.12 (s, 6H, 2 x SiCH_3), −0.02 (s, 3H, SiCH_3), −0.14 (s, 3H, SiCH_3). ^{13}C NMR (90 MHz, $CDCl_3$) δ (ppm) 140.7 (1C, C-6), 102.8 (1C, C-5), 87.8 (1C, C-1′), 79.5, 63.8 (1C, C-5′), 47.2 (1C, C-3′), 35.4 (1C, *i*-Pr *C*H), 27.4 (1C, S*C*H$_2$), 26.1, 25.7 (6C, 2 x SiC(*C*H$_3$)$_3$), 23.3 (2C, 2 x *i*-Pr *C*H$_3$), −4.5, −4.6, −5.3, −5.5 (4C, *4* x SiCH_3). MALDI-TOF MS: m/z calcd for $C_{25}H_{48}N_2NaO_5SSi_2$ $[M+Na]^+$ 567.2715, found 567.2716.

1-[3′-Deoxy-3′-C-(*i*-propyl-sulfanylmethyl)-2′-*O*-(*tert*-butyldimethylsilyl)-β-D-xylofuranosyl]-uracil (12)

6 (220 mg, 0.4 mmol) was dissolved in THF (3 mL) and cooled to 0 °C. Then, the mixture of TFA (2 mL) and H_2O (2 mL) was added and stirred vigorously at 0 °C for 2 h. The reaction mixture was diluted with sat. aq. $NaHCO_3$ (100 mL) and extracted with CH_2Cl_2 (3 × 50 mL). The organic phase was dried over Na_2SO_4, filtered and concentrated under reduced pressure. The residue was purified by flash chromatography (CH_2Cl_2/aceton e 9/1) to give **6** (81 mg, 48 %) as a colorless syrup. $[\alpha]_D = +61.4$ ($c = 0.14$, $CHCl_3$), Rf = 0.16 (CH_2Cl_2/acetone 9/1), ^{1}H NMR (360 MHz, $CDCl_3$) δ (ppm) 8.98 (s, 1H, N*H*), 7.61 (d, $J = 8.1$ Hz, 1H, H-6), 5.74 (dd, $J = 8.1$, 2.1 Hz, 1H, H-5), 5.42 (d, $J = 6.6$ Hz, 1H, H-1′), 4.48 (dd, $J = 9.1$, 6.7 Hz, 1H, H-2′), 4.33 (d, $J = 8.3$ Hz, 1H, H-4′), 3.90 (dt, $J = 18.9$, 8.7 Hz, 2H, H-5′ab), 3.16 (s, 1H, O*H*), 2.93 (dd, $J = 13.4$, 6.7 Hz, 1H, SCH_2a), 2.85 – 2.73 (m, 2H, SCH_2b, H-3′), 2.59 (ddd, $J =$ 19.8, 9.0, 4.4 Hz, 1H, *i*-Pr CH), 1.25 (dd, $J = 6.7$, 3.7 Hz, 6H, 2 x *i*-Pr CH_3), 0.83 (s, 9H, *t*-Bu), 0.03, −0.12 (2 x s, 2 × 3H, SiCH_3). ^{13}C NMR (90 MHz, $CDCl_3$) δ (ppm) 163.0, 150.5 (2C, C-2, C-4), 142.8 (1C, C-6), 102.8 (1C, C-5), 93.3 (1C, C-1′), 80.1, 75.6 (2C, C-2′, C-4′), 62.3 (1C, C-5′), 47.1 (1C, C-3′), 35.4 (1C, *i*-Pr *C*H), 27.5 (1C, S*C*H$_2$), 25.6 (3C, SiC(*C*H$_3$)$_3$), 23.2, 23.2 (2C, 2 x *i*-Pr *C*H$_3$), 17.7 (1C, *t*-Bu C_q), −4.5, −4.7 (2C, *2* x SiCH_3). MALDI-TOF MS: m/z calcd for $C_{19}H_{34}N_2NaO_5SSi$ $[M+Na]^+$ 453.1850, found 453.1858.

1-[3′-Deoxy-3′-C-(*i*-propyl-sulfanylmethyl)-5′-*n*-butyryl-2′-*O*-(*tert*-butyldimethylsilyl)-β-D-xylofuranosyl]-uracil (18)

12 (54 mg, 0.13 mmol) was dissolved in dry pyridine (1 mL) and butyryl chloride (16 μL, 0.16 mmol, 1.2 equiv.) was added and stirred overnight. The reaction mixture was diluted with CH_2Cl_2 (10 0 mL) and extracted with 10 % aq. $NaHSO_4$ (3 × 50 mL) and brine (1 × 50 mL). The organic phase was dried over Na_2SO_4, filtered and concentrated under reduced pressure. The residue was purified by flash chromatography (hexane/acetone 9/1) to give **18** (65 mg, 60 %) as a colorless syrup. $[\alpha]_D = +53.3$ ($c = 0.12$, $CHCl_3$), Rf = 0.7 (CH_2Cl_2/acetone 9/1), ^{1}H NMR (360 MHz, $CDCl_3$) δ (ppm) 9.43 (s, 1H, N*H*), 7.54 (d, $J = 8.2$ Hz, 1H, H-6), 5.73 (t, $J = 6.9$ Hz, 2H, H-1′, H-5), 4.53 (dd, $J = 5.3$, 2.7 Hz, 1H, H-4′), 4.45 (dd, $J = 13.4$, 4.4 Hz, 1H, H-5′a), 4.28 – 4.22 (m, 2H, H-5′b, H-2′), 2.85 (dt, $J = 13.4$, 6.7 Hz, 1H), 2.58 – 2.39 (m, 4H), 2.31 (t, $J = 7.4$ Hz, 2H, CH$_3$CH$_2$CH_2CO), 1.72 – 1.61 (m, 2H, CH$_3$CH_2CH$_2$CO), 1.20 (dd, $J =$ 6.6, 1.7 Hz, 6H, 2 x *i*-Pr CH_3), 0.94 (t, $J = 7.4$ Hz, 3H, CH_3CH$_2$CH$_2$CO), 0.84 (s, 9H, *t*-Bu), 0.04, −0.01 (2 x s, 2 × 3H, SiCH$_3$). ^{13}C NMR (90 MHz, $CDCl_3$) δ (ppm) 173.0 (1C, CH$_3$CH$_2$CH$_2$*C*O), 163.3, 150.5 (2C, C-2, C-4), 139.5 (1C, C-6), 102.7 (1C, C-5), 90.7 (1C, C-1′), 78.2, 78.0 (2C, C-2′, C-3′), 63.6 (1C, C-5′), 47.5 (1C, C-3′), 36.3 (1C, CH$_3$CH$_2$*C*H$_2$CO), 35.6 (1C, *i*-Pr *C*H), 27.4 (1C, S*C*H$_2$), 25.7 (3C, SiC(*C*H$_3$)$_3$), 23.3, 23.2 (2C, 2 x *i*-Pr *C*H$_3$), 18.5 (2C, *t*-Bu C_q, CH$_3$*C*H$_2$CH$_2$CO), 13.9 (1C, *C*H$_3$CH$_2$CH$_2$CO), −4.6, −4.7 (2C, *2* x SiCH_3). MALDI-TOF MS: m/z calcd for $C_{23}H_{40}N_2NaO_6SSi$ $[M+Na]^+$ 523.2269, found 523.2267.

1-[3′-Deoxy-3′-C-(*i*-propyl-sulfanylmethyl)-5′-*n*-butyryl-β-D-xylofuranosyl]-uracil (24)

18 (30 mg, 0.0 6 mmol) was dissolved in 90 % aq. TFA and stirred for 5 h at r.t. The reaction mixture was diluted with sat. aq. $NaHCO_3$ (50 mL) and extracted with CH_2Cl_2 (3 × 50 mL). The organic phase was dried over Na_2SO_4, filtered and evaporated under reduced pressure. The residue was purified by flash chromatography (CH_2Cl_2/acetone 95/5) to give **24** (23 mg, 78 %) as a colorless syrup. $[\alpha]_D = +75.33$ ($c = 0.15$, $CHCl_3$), Rf = 0.46 (CH_2Cl_2/acetone 9/1), ^{1}H NMR (360 MHz, $CDCl_3$) δ (ppm) 7.60 (d, $J = 8.2$ Hz, 1H, H-6), 5.70 (d, $J = 8.2$ Hz, 1H, H-5), 5.62 (d, $J = 4.7$ Hz, 1H, H-1′), 4.70 – 4.59 (m, 1H, H-4′), 4.29–4.35 (m, 2H, H-5′ab) 4.15 (dd, $J = 8.2$, 4.9 Hz, 1H, H-2′), 2.94 (dd, $J = 13.3$, 6.7 Hz, 1H, SCH_2a), 2.89 – 2.81 (m, 1H, H-3′), 2.75 (dd, $J = 15.0$, 8.3 Hz, 1H, SCH_2b), 2.54 – 2.42 (m, 1H, *i*-Pr C*H*), 2.22 (dd, $J = 14.5$, 7.3 Hz, 2H, CH$_3$CH$_2$CH_2CO), 1.60 (dd, $J = 14.7$, 7.4 Hz, 2H, CH$_3$CH$_2$CH$_2$CO), 1.24 (d, $J = 6.6$ Hz, 6H, 2 x *i*-Pr CH_3), 0.91 (t, $J = 7.4$ Hz, 3H, CH_3CH$_2$CH$_2$CO). ^{13}C NMR (90 MHz, $CDCl_3$) δ (ppm) 172.9 (1C, CH$_3$CH$_2$CH$_2$*C*O), 163.7, 151.9 (2C, C-2, C-4), 139.6 (1C, C-6), 102.0 (1C, C-5), 93.3 (1C, C-1′), 80.1, 79.7 (2C, C-2′, C-4′), 63.6 (1C, C-5′), 47.0 (1C, C-3′), 36.3 (1C, CH$_3$CH$_2$*C*H$_2$CO), 35.8 (1C, *i*-Pr *C*H), 28.0 (1C, S*C*H$_2$), 18.4 (2C, CH$_3$*C*H$_2$CH$_2$CO), 23.4 (2C, 2 x *i*-Pr *C*H$_3$), 13.8 (1C, 1C, *CH$_3$*CH$_2$CH$_2$CO). MALDI-TOF MS: m/z calcd for $C_{17}H_{26}N_2NaO_6S$ $[M+Na]^+$ 409.1404, found 409.1400.

1-[3′-Deoxy-3′-C-(*t*-butyl-sulfanylmethyl)-2′,5′-di-*O*-

(*tert*-butyldimethylsilyl)-β-D-xylofuranosyl] -uracil (7)

1 (234 mg, 0.5 mmol) was dissolved in toluene (2 mL) and *t*-BuSH (451 μL, 4.0 mmol, 8.0 equiv.) and DPAP (12.8 mg, 0.05 mmol, 0.1 equiv.) were added and cooled to 0 °C. The reaction mixture was irradiated at 0 °C for 6 × 15 min. The solvent was evaporated under reduced pressure and the crude product was purified by flash chromatography (hexane/acetone 9/1) to give **7** (207 mg, 74 %, D-xylo:D-ribo ratio = 16:1) as a colorless syrup. $[\alpha]_D = +60.7$ ($c = 0.14$, $CHCl_3$), Rf = 0.26 (hexane/acetone 9/1), ^{1}H NMR (360 MHz, $CDCl_3$) δ (ppm) 8.54 (s, 1H, N*H*), 7.98 (d, $J = 8.2$ Hz, 1H, H-6), 5.91 (d, $J = 6.7$ Hz, 1H, H-1′), 5.68 (dd, $J = 8.1$, 2.1 Hz, 1H, H-5), 4.24 (d, $J = 7.8$ Hz, 1H, H-4′), 4.12 (dd, $J = 9.2$, 6.8 Hz, 1H, H-2′), 3.86 (dt, $J = 11.9$, 7.0 Hz, 2H, H-5′ab), 2.76 – 2.72 (m, 1H, SCH_2a), 2.70 – 2.59 (m, 2H, H-3′, SCH_2b), 1.30 (s, 9H, S-*t*-Bu), 0.93 (s, 9H, Si-*t*-Bu), 0.84 (s, 9H, Si-*t*-Bu), 0.12 (d, $J = 1.8$ Hz, 6H, 2 x SiCH_3), −0.00 (s, 3H, SiCH_3), −0.13 (s, 3H, SiCH_3). ^{13}C NMR (90 MHz, $CDCl_3$) δ (ppm) 162.9, 150.6 (C-2, C-4), 140.7, 102.8 (2C, C-5, C-6), 87.8 (1C, C-1′), 79.5, 77.6 (2C, C-2′, C-4′), 63.9 (1C, C-5′), 48.2 (1C, C-3′), 31.0 (3C, SC(CH_3)$_3$), 26.1, 25.7 (6C, 2 x SiC(CH_3)$_3$), 25.5, −4.4, −4.6, −5.3, −5.5 (4C, *4* x SiCH_3). MALDI-TOF MS: m/z calcd for $C_{26}H_{50}N_2NaO_5SSi_2$ $[M+Na]^+$ 581.2871, found 581.2874.

1-[3′-Deoxy-3′-C-(*t*-butyl-sulfanylmethyl)-2′-*O*-(*tert*-butyldimethylsilyl)-β-D-xylofuranosyl] -uracil (13)

7 (178 mg, 0.32 mmol) was dissolved in THF (3 mL) and cooled to 0 °C. Then, the mixture of TFA (2 mL) and H_2O (2 mL) was added and stirred vigorously at 0 °C for 2 h. The reaction mixture was diluted with sat. aq. $NaHCO_3$ (100 mL) and extracted with CH_2Cl_2 (3 × 50 mL). The organic phase was dried over Na_2SO_4, filtered and concentrated under reduced pressure. The residue was purified by flash chromatography (CH_2Cl_2/acetone 9/1) to give **13** (92 mg, 68 %) as a colorless syrup. $[\alpha]_D = +50.0$ ($c = 0.1$, $CHCl_3$), Rf = 0.2 (CH_2Cl_2/acetone 9/1), ^{1}H NMR (360 MHz, $CDCl_3$) δ (ppm) 8.82 (s, 1H, N*H*), 7.61 (d, $J = 8.1$ Hz, 1H, H-6), 5.74 (dd, $J = 8.1$, 2.1 Hz, 1H, H-5), 5.41 (d, $J = 6.6$ Hz, 1H, H-1′), 4.49 (dd, $J = 9.1$, 6.6 Hz, 1H, H-2′), 4.30 (d, $J = 8.4$ Hz, 1H, H-4′), 3.95 – 3.81 (m, 2H, H-5′ab), 3.14 (dd, $J = 6.2$, 3.2 Hz, 1H, O*H*), 2.84 (t, $J = 11.7$ Hz, 1H, SCH_2a), 2.75 (dd, $J = 11.9$, 3.9 Hz, 1H, SCH_2b), 2.66 – 2.52 (m, 1H, H-3′), 1.30 (s, 9H, S-*t*-Bu), 0.84 (s, 9H, Si-*t*-Bu), 0.04 (s, 3H, SiCH_3), −0.11 (s, 3H, SiCH_3). ^{13}C NMR (90 MHz, $CDCl_3$) δ (ppm) 163.0, 150.6 (12C, C-2, C-4), 142.9 (1C, C-6), 102.9 (1C, C-5), 93.4 (1C, C-1′), 80.2, 75.8 (2C, C-2′, C-4′), 62.5 (1C, C-5′), 47.8 (1C, C-3′), 30.9, 25.7 (6C, 2 x C(CH_3)$_3$), 25.6, −4.4, −4.7 (2C, *2* x SiCH_3). MALDI-TOF MS: m/z calcd for $C_{20}H_{36}N_2NaO_5SSi$ $[M+Na]^+$ 467.2006, found 467.2014.

1-[3′-Deoxy-3′-C-(*t*-butyl-sulfanylmethyl)-5′-*n*-butyryl-2′-*O*-(*tert*-butyldimethylsilyl)-β-D-xylofuranosyl] -uracil (19)

13 (69 mg, 0.16 mmol) was dissolved in dry pyridine (1 mL) and butyryl chloride (19 μL, 0.19 mmol, 1.2 equiv.) was added and stirred overnight. The reaction mixture was diluted with CH_2Cl_2 (10 0 mL) and extracted with 10 % aq. $NaHSO_4$ (3 × 50 mL) and brine (1 × 50 mL). The organic phase was dried over Na_2SO_4, filtered and concentrated under reduced pressure. The residue was purified by flash chromatography (hexane/acetone 9/1) to give **19** (58 mg, 73 %) as a colorless syrup. $[\alpha]D = +58.0$ ($c = 0.15$, $CHCl_3$), Rf = 0.16 (CH_2Cl_2/acetone 8/2), ^{1}H NMR (360 MHz, $CDCl_3$) δ (ppm) 9.51 (s, 1H, N*H*), 7.56 (d, $J = 8.2$ Hz, 1H, H-6), 5.73 (dd, $J = 10.5$, 3.3 Hz, 2H, H-1′, H-5), 4.52 (dd, $J = 5.6$, 2.7 Hz, 1H, H-4′), 4.46 (dd, $J = 12.1$, 5.7 Hz, 1H, H-5′a), 4.30 – 4.22 (m, 2H, H-5′b, H-2′), 2.53 – 2.42 (m, 3H, H-3′, SCH_2), 2.31 (t, $J = 7.4$ Hz, 2H, $CH_3CH_2CH_2CO$), 1.65 (dt, $J = 14.7$, 7.4 Hz, 2H, $CH_3CH_2CH_2CO$), 1.24 (s, 9H, S-*t*-Bu), 0.94 (t, $J = 5.2$ Hz, 3H, $CH_3CH_2CH_2CO$), 0.84 (s, 9H, Si-*t*-Bu), 0.05, −0.01 (2 x s, 2 × 3H, 2 x SiCH_3). ^{13}C NMR (90 MHz, $CDCl_3$) δ (ppm) 172.9 (1C, $CH_3CH_2CH_2CO$)163.3, 150.5 (2C, C-2, C-4), 139.4 (1C, C-6), 102.6 (1C, C-5), 90.5 (1C, C-1′), 78.3, 78.0 (2C, C-2′, C-4′), 63.6 (1C, C-5′), 47.7 (1C, C-3′), 36.3 (1C, $CH_3CH_2CH_2CO$), 25.3 (1C, SCH_2), 30.7, 25.6, (6C, 2 x C(CH_3)$_3$), 18.5 (3C, $CH_3CH_2CH_2CO$, 2 x *t*-Bu C_q), 13.7 (1C, $CH_3CH_2CH_2CO$), −4.64, −4.7 (2C, *2* x SiCH_3). MALDI-TOF MS: m/z calcd for $C_{24}H_{42}N_2NaO_6SSi$ $[M+Na]^+$ 537.2425, found 537.2433.

1-[3′-Deoxy-3′-C-(*t*-butyl-sulfanylmethyl)-5′-*n*-butyryl-β-D-xylofuranosyl] -uracil (25)

19 (46 mg, 0. 9 mmol) was dissolved in 90 % aq. TFA and stirred for 5 h at r.t. The reaction mixture was diluted with sat. aq. $NaHCO_3$ (50 mL) and extracted with CH_2Cl_2 (3 × 50 mL). The organic phase was dried over Na_2SO_4, filtered and evaporated under reduced pressure. The residue was purified by flash chromatography (hexane/acetone 7/3) to give **25** (28 mg, 80 %) as a colorless syrup. $[\alpha]_D = +95.0$ ($c = 0.1$, $CHCl_3$), Rf = 0.18 (hexane/acetone 7/3), ^{1}H NMR (360 MHz, $CDCl_3$) δ (ppm) 10.26 (s, 1H, N*H*), 7.64 (d, $J = 8.2$ Hz, 1H, H-6), 5.73 (d, $J = 8.2$ Hz, 1H, H-5), 5.67 (d, $J = 5.0$ Hz, 1H, H-1′), 4.68 – 4.58 (m, 2H, H-4′, O*H*), 4.36 (qd, $J = 12.6$, 3.6 Hz, 2H, H-5′ab), 4.19 (dd, $J = 8.1$, 5.1 Hz, 1H, H-2′), 2.89 (dd, $J = 11.7$, 5.2 Hz, 1H, SCH_2a), 2.84 – 2.71 (m, 1H, H-3′), 2.49 (t, $J = 11.1$ Hz, 1H, SCH_2b), 2.26 (td, $J = 7.4$, 5.3 Hz, 2H, $CH_3CH_2CH_2CO$), 1.64 (dq, $J = 14.7$, 7.4 Hz, 2H, $CH_3CH_2CH_2CO$), 1.31 (s, 9H, *t*-Bu), 0.95 (t, $J = 7.4$ Hz, 3H, $CH_3CH_2CH_2CO$). ^{13}C NMR (90 MHz, $CDCl_3$) δ (ppm) 172.9 (1C, $CH_3CH_2CH_2CO$), 163.8, 151.9 (2C, C-2, C-4), 139.6 (1C, C-6), 101.9 (1C, C-5), 93.1 (1C, C-1′), 80.2, 79.6 (2C, C-2′, C-4′), 63.6 (1C, C-5′), 47.1 (1C, C-3′), 30.8 (3C, C(CH_3)$_3$), 36.3 (1C, $CH_3CH_2CH_2CO$), 25.8 (1C, SCH_2), 18.4 (2C, $CH_3CH_2CH_2CO$, *t*-BuC_q), 13.8 (1C, $CH_3CH_2CH_2CO$). MALDI-TOF MS: m/z calcd for $C_{18}H_{28}N_2NaO_6S$ $[M+Na]^+$ 423.1566, found 423.1555

1-[3′-Deoxy-3′-C-(2,3,4,6-tetra-*O*-acetyl-β-D-glucopyranose-1-yl-sulfanylmethyl)-2′-*O*-(*tert*-butyldimethylsilyl)-β-D-xylofuranosyl] -uracil (14)

8 (325 mg, 0.39 mmol) was dissolved in THF (3 mL) and cooled to 0 °C. Then, the mixture of TFA (2 mL) and H_2O (2 mL) was added and stirred vigorously at 0 °C for 2 h. The reaction mixture was diluted with sat. aq. $NaHCO_3$ (100 mL) and extracted with CH_2Cl_2 (3 × 50 mL). The organic phase was dried over Na_2SO_4, filtered and concentrated under reduced pressure. The residue was purified by flash chromatography (CH_2Cl_2/acetone 9/1→ 8/2) to give **14** (172 mg, 61 %) as a colorless syrup. $[\alpha]_D = +4.5$ ($c = 0.2$, $CHCl_3$), Rf = 0.2 (CH_2Cl_2/acetone 9/1), ^{1}H NMR (360 MHz, $CDCl_3$) δ (ppm) 8.81 (s, 1H, N*H*), 7.78 (d, $J = 8.1$ Hz, 1H, H-6), 5.75 (d, $J = 8.0$ Hz, 1H, H-5), 5.57 (d, $J = 6.7$ Hz, 1H, H-1′), 5.20 (t, $J = 9.4$ Hz, 1H, H-3′′), 5.08 – 4.93 (m, 2H, H-4′′, H-2′′), 4.45 – 4.34 (m, 2H), 4.29 (dd, $J = 12.4$, 5.3 Hz, 2H), 4.14 (d, $J = 12.3$ Hz, 1H), 3.91 (dd, $J = 12.0$, 6.2 Hz, 1H), 3.81 (d, $J = 12.1$ Hz, 1H), 3.72 (ddd, $J = 9.8$, 5.5, 1.9 Hz, 1 H, H-5′′), 3.18 (d, $J = 4.3$ Hz, 1H), 3.03 – 2.90 (m, 2H, SCH_2), 2.60 (ddd, $J = 13.6$, 9.9, 4.7 Hz, 1H, H-3′), 2.10, 2.03, 2.02, 1.98 (4 x s, 4 × 3H, 4 x AcCH_3), 0.84 (s, 9H, *t*-Bu), 0.06, −0.12 (2 x s, 2 × 3H, SiCH_3). ^{13}C NMR (90 MHz, $CDCl_3$) δ (ppm) 171.1, 170.3, 169.6, 169.4 (4C, 4 x Ac*C*O), 163.0, 150.7 (2C, C-2, C-4), 142.5 (1C, C-6), 103.1 (1C, C-5), 91.7 (1C, C-1′), 83.6 (1C, C-1′′), 79.7, 76.4, 76.2 (3C, C-2′, C-4′, C-5′′), 73.7 (1C, C-3′′), 69.4 (1C, C-2′′), 68.4 (1C, C-4′′), 62.2 (2C, C-5′, C-6′′), 46.8 (1C, C-3′), 26.7 (1C, SCH_2), 25.7 (3C, SiC(CH_3)$_3$), 20.9, 20.8, 20.7 (4C, 4 x AcCH_3), −4.4, −4.7 (2C, *2* x SiCH_3). MALDI-TOF MS: m/z calcd for $C_{30}H_{46}N_2NaO_{14}SSi$ $[M+Na]^+$ 741.2331, found 741.2328.

1-[3′-Deoxy-3′-C-(2,3,4,6-tetra-*O*-acetyl-β-D-glucopyranose-1-yl-sulfanylmethyl)-5′-*n*-butyryl-2′-*O*-(*tert*-butyldimethylsilyl)-β-D-xylofuranosyl] -uracil (20)

14 (133 mg, 0.19 mmol) was dissolved in dry pyridine (1 mL) and butyryl chloride (23 μL, 0.22 mmol, 1.2 equiv.) was added and stirred overnight. The reaction mixture was diluted with CH_2Cl_2 (10 0 mL) and extracted with 10 % aq. $NaHSO_4$ (3 × 50 mL) and brine (1 × 50 mL). The organic phase was dried over Na_2SO_4, filtered and concentrated under reduced pressure. The residue was purified by flash chromatography (hexane/acetone 9/1) to give **20** (107 mg, 73 %) as a white foam. $[\alpha]_D = +22.7$ ($c = 0.13$, $CHCl_3$), Rf = 0.28 (hexane/acetone 7/3), ^{1}H NMR (400 MHz, $CDCl_3$) (ppm) δ 7.57 (d, $J = 8.2$ Hz, 1H, H-6), 5.80 (d, $J = 8.1$ Hz, 1H, H-5), 5.76 (d, $J = 4.7$ Hz, 1H, H-1′), 5.24 (t, $J = 9.4$ Hz, 1H, H-3′′), 5.06 (t, $J = 9.8$ Hz, 1H, H-4′′), 4.99 (t, $J = 9.7$ Hz, 1H, H-2′′), 4.58 (ddd, $J = 7.3$, 5.6, 3.3 Hz, 1H, H-4′), 4.48 – 4.41 (m, 1H, H-1′′), 4.31 (dd, $J = 12.3$, 3.2 Hz, 1H, H-5′a), 4.26 – 4.14 (m, 4H, H-2′, H-5′b, H-6′′ab), 3.75 (ddd, $J = 10.0$, 5.1, 2.3 Hz, 1H, H-5′′), 2.74 (ddd, $J = 27.7$, 12.2, 8.1 Hz, 2H, SCH_2), 2.62 (dt, $J = 15.0$, 7.5 Hz, 1H, H-3′), 2.37 (t, $J = 7.4$ Hz, 2H, COCH_2CH$_2$CH$_3$), 2.13, 2.06, 2.05, 2.03 (4 x s, 4 × 3H, 4 x AcCH_3), 1.71

(dq, J = 14.8, 7.4 Hz, 2H, $COCH_2CH_2CH_3$), 1.00 (t, J = 7.4 Hz, 3H, $COCH_2CH_2CH_3$), 0.90 (s, 9H, *t*-Bu), 0.11, 0.03 (2 x s, 2 × 3H, 2 x $SiCH_3$). ^{13}C NMR (100 MHz, $CDCl_3$) δ (ppm) 172.9, 170.2, 169.6, 169.5 (4C, 4 x Ac*C*O), 165.1 (1C, $CH_3CH_2CH_2CO$), 162.8, 150.3 (2C, C-2, C-4), 139.6 (1C, C-6), 102.9 (1C, C-5), 90.7 (1C, C-1′), 83.3 (1C, C-1′′), 78.3, 77.7 (2C, C-2′, C-4′), 76.5 (1C, C-5′′), 73.6 (1C, C-3′′), 69.5 (1C, C-2′′), 68.3 (1C, C-4′′), 63.5, 62.3 (2C, C-5′, C-6′′), 47.6 (1C, C-3′), 36.3 (1C, $CH_3CH_2CH_2CO$), 26.5 (1C, SCH_2), 25.7 (3C, $SiC(CH_3)_3$), 20.9, 20.7 (4C, 4 x AcCH_3), 18.6 (2C, $CH_3CH_2CH_2CO$, *t*-Bu C_q), 13.8 (1C, $CH_3CH_2CH_2CO$), −4.6 (2C, *2* x $SiCH_3$). MALDI-TOF MS: m/z calcd for $C_{34}H_{52}N_2NaO_{15}SSi$ $[M+Na]^+$ 811.2750, found 811.2758.

1-[3′-Deoxy-3′-C-(2,3,4,6-tetra-*O*-acetyl-β-D-glucopyranose-1-yl-sulfanylmethyl)-5′-*n*-butyryl-β-D-xylofuranosyl]-uracil (26)

20 (85 mg, 0.1 1 mmol) was dissolved in 90 % aq. TFA and stirred for 8 h at r.t. The reaction mixture was diluted with sat. aq. $NaHCO_3$ (50 mL) and extracted with CH_2Cl_2 (3 × 50 mL). The organic phase was dried over Na_2SO_4, filtered and evaporated under reduced pressure. The residue was purified by flash chromatography (hexane/acetone 6/4) to give **26** (56 mg, 75 %) as white solid. $[\alpha]_D$ = +45.0 (c = 0.13, $CHCl_3$), Rf = 0.28 (hexane/acetone 7/3), ^{1}H NMR (500 MHz, $CDCl_3$) δ (ppm) 9.93 (s, 1H, N*H*), 7.61 (d, J = 8.2 Hz, 1H, H-6), 5.75 (d, J = 8.2 Hz, 1H, H-5), 5.61 (d, J = 4.9 Hz, 1H, H-1′), 5.24 (t, J = 9.4 Hz, 1H, H-3′′), 5.06 (d, J = 9.9 Hz, 1H, H-4′′), 5.00 (t, J = 9.7 Hz, 1H, H-2′′), 4.70 (dt, J = 7.6, 3.7 Hz, 1H, H-4′), 4.56 (d, J = 10.1 Hz, 1H, H-1′′), 4.42 (s, 1H, O*H*), 4.36 (dd, J = 12.7, 3.0 Hz, 1H, H-5′a), 4.29 (dd, J = 12.7, 4.5 Hz, 1H, H-5′b), 4.19 (d, J = 3.9 Hz, 2H, H-6′′ab), 4.17 – 4.14 (m, 1H, H-2′), 3.79 (dt, J = 10.1, 3.9 Hz, 1H, H-5′′), 3.00 (dd, J = 13.1, 5.9 Hz, 1H, SCH_2a), 2.90 – 2.82 (m, 1H, H-3′), 2.70 (dd, J = 13.0, 10.0 Hz, 1H, SCH_2b), 2.33 – 2.19 (m, 2H, $CH_3CH_2CH_2CO$), 2.10, 2.05, 2.04, 2.01 (4 x s, 4 × 3H, 4 x AcCH_3), 1.63 (h, J = 7.4 Hz, 2H, $CH_3CH_2CH_2CO$), 0.94 (t, J = 7.4 Hz, 3H, $CH_3CH_2CH_2CO$). ^{13}C NMR (120 MHz, $CDCl_3$) δ (ppm) 172.8, 170.9, 170.2, 169.6 (5C, 4 X AcCO, $CH_3CH_2CH_2CO$), 163.7, 151.8 (2C, C-2, C-4), 139.6 (1C, C-6), 102.1 (1C, C-5), 93.3 (1C, C-1′), 83.9 (1C, C-1′′), 79.9 (1C, C-2′), 79.5 (1C, C-4′), 76.1 (1C, C-5′′), 73.7 (1C, C-3′′), 69.9 (1C, C-2′′), 68.4 (1C, C-4′′), 63.5 (1C, C-5′), 62.3 (1C, C-6′′), 47.3 (1C, C-3′), 36.2 (1C, $CH_3CH_2CH_2CO$), 27.9 (1C, SCH_2), 20.8, 20.8, 20.7 (4C, 4 x AcCH_3), 18.4 (1C, $CH_3CH_2CH_2CO$). MALDI-TOF MS: m/z calcd for $C_{28}H_{38}N_2NaO_{15}S$ $[M+Na]^+$ 697.1885 found 697.1883.

2.2. Antiviral assays

2.2.1. Anti-SARS-CoV-2 determination by cytopathic effect- and immunofluorescence-based assays

Anti-SARS-CoV-2 activity of all compounds was in the first step tested in Vero E6 cells (5000 cells/25 μL) in 384-well plate format. Compounds were added to the cells, after one hour, cells were infected with SARS-CoV-2 strain hCoV-19/Czech Republic/NRL_6632_2/2020 at MOI 0.05. Cells were incubated for 72 h in CO_2 incubator set to 37 °C, and after incubation cytopathic effect (CPE) was analyzed by XTT colorimetric assay. Briefly, 50 μL of 50:1 mixture of XTT labeling reagent (1 mg/mL) and PMS electron-coupling reagent (0.383 mg/mL) was added to the wells and incubated for 4 h in 37 °C in 5 % CO_2. Formation of orange formazan dye was measured in EnVision plate reader.

Anti-SARS-CoV-2 activity of selected compounds was measured by immunofluorescence asssay (IF) in Vero E6 cells (15,000 cells/100 μL) in 96-well plate format. Compounds were tested using 2-fold dilution. Compounds were added to the cells, after one hour, cells were infected with SARS-CoV-2 (MOI 0.05). Cells were incubated for 72 h in CO_2 incubator set to 37 °C and after incubation IF assay was performed. Briefly, medium was washed out, cells were fixed using 4 % PFA, cell membranes were perforated with 0.2 % Triton-X100 and SARS-CoV-2 was labeled with mouse anti-SARS-CoV-2 antibody, anti-mouse antibody conjugated with Cy-3 fluorophore and signal was detected using fluorescent microscope.

Four compounds (**3, 4, 7, 19**) were further tested for anti-SARS-CoV-2 activity in human Calu3 cells (15.000 cells/25 μL) in 384-well plate format. EC_{50} was measured in CPE assay using 2-fold dilution. Compounds were added to the cells, after one hour, cells were infected with SARS-COV-2 virus (MOI 0.05). Cells were incubated for 72 h in CO_2 incubator set to 37 °C and after incubation cytopathic effect (CPE) was analyzed by XTT colorimetric assay as above. Tempest liquid dispenser system (Formulatrix) was used for all dispensing steps.

2.2.2. Anti-CHIKV and anti-SINV determination by cytopathic effect-based assays

Antiviral activity of the compounds were measured against CHIKV (Guatemala) and SINV (UVE/SINV/2017/DZ/P29) viruses. Vero E6 cells (35 000 cell/well) were seeded in 96-well plate format and incubated (37 °C, 5 % CO_2) the day before the infection. For screening, the compounds were diluted in halving series based on the CC_{50} values. The tested components were added in parallel with the infection of the cells. We infected the cells with 0.1 MOI CHIKV for 1 hour and 0.01 MOI SINV for 30 min. After the infection the cells were incubated (37 °C, 5 % CO_2) for 3 days (CHIKV) and for 2 days (SINV). The antiviral activity of the compounds was measured by microscopic observation. The active compounds were further tested with MTT (3-[4,5-Dimethylthiazol-2-yl]−2,5-diphenyltetrazolium bromide) colorimetric cell viability assay to determine the EC_{50} values. Vero E6 cells (35 000 cell/well) were seeded in 96-well plate format and incubated (37 °C, 5 % CO_2) the day before the infection. The cells were treated with the compounds diluted at indicated concentrations (based on the results of the sreening) parallel with the infection. The control group was treated with an equal concentration of DMSO. After one hour of CHIKV infection at 0.1 MOI and 30 min of the SINV infection at 0.01 MOI, the supernatant was discarded, and the cells were incubated for 3 days (CHIKV) and for 2 days (SINV) with the compounds. Following the appropriate incubation time and microscopic examination, our measurements were carried out using 50 μL MTT working solution per 100 μL sample. The absorbance was measured at 570 nm with Crocodile 5in1 mini Workstation (Berthold, Germany). Three biological replicates of each concentration were used.

2.2.3. Cytotoxicity in VeroE6 and Calu-3 cells (XTT and MTT assays - CC_{50} measurement)

In the case of SARS-CoV-2, cytotoxity was masured in Vero E6 cells (5000 cells/25 μL) and Calu-3 cells (15,000 cells/25 μL) in 384-well plate format. Compound cytotoxicity was tested at the same concentration range as EC_{50} measurements. Cytotoxicity was detected after 72 h using XTT colorimetric assay as above.

In the case of CHIKV and SINV viruses, cytotoxicity was measured in Vero E6 cells (35,000 cell/well) in 96-well plate format. Cytotoxicity was detected after 72 h using MTT colorimetric assay as above.

3. Results and discussion

3.1. Chemical synthesis

Our preliminary studies showed that the introduction of an *n*-butylthio group at the 3′-position of a uridine derivative conferred antiviral activity to the molecule without toxic effects, while larger thio substituents at the 3′-position significantly increased cytotoxicity. Therefore, we introduced normal and branched alkyl chains of similar size to *n*-butyl, such as ethyl, *i*-propyl, *tert*-butyl and *n*-hexyl groups, to the 3′-position of uridine to obtain compounds with good antiviral activity profiles (**3, 5**–**7**, Scheme 1). In addition, we also prepared the already known derivatives containing *n*-butyl (**4**) and 1-thioglucose (**8**) substituents. These compounds were prepared by UV-light initiated thiol-ene coupling reaction between 3-exomethylene uridine **1** and thiols **2a-d** using DPAP (2,2-dimethoxy-2-phenylacetophenone) as photoinitiator. The photochemical thiol-ene click reaction is a radical chain reaction that yields an anti-Markovnikov product in a completely regioselective manner (Scheme 1). (Cramer et al. 2004; Hoyle and Bowman, 2010; Dondoni and Marra, 2012) In the case of endo- and

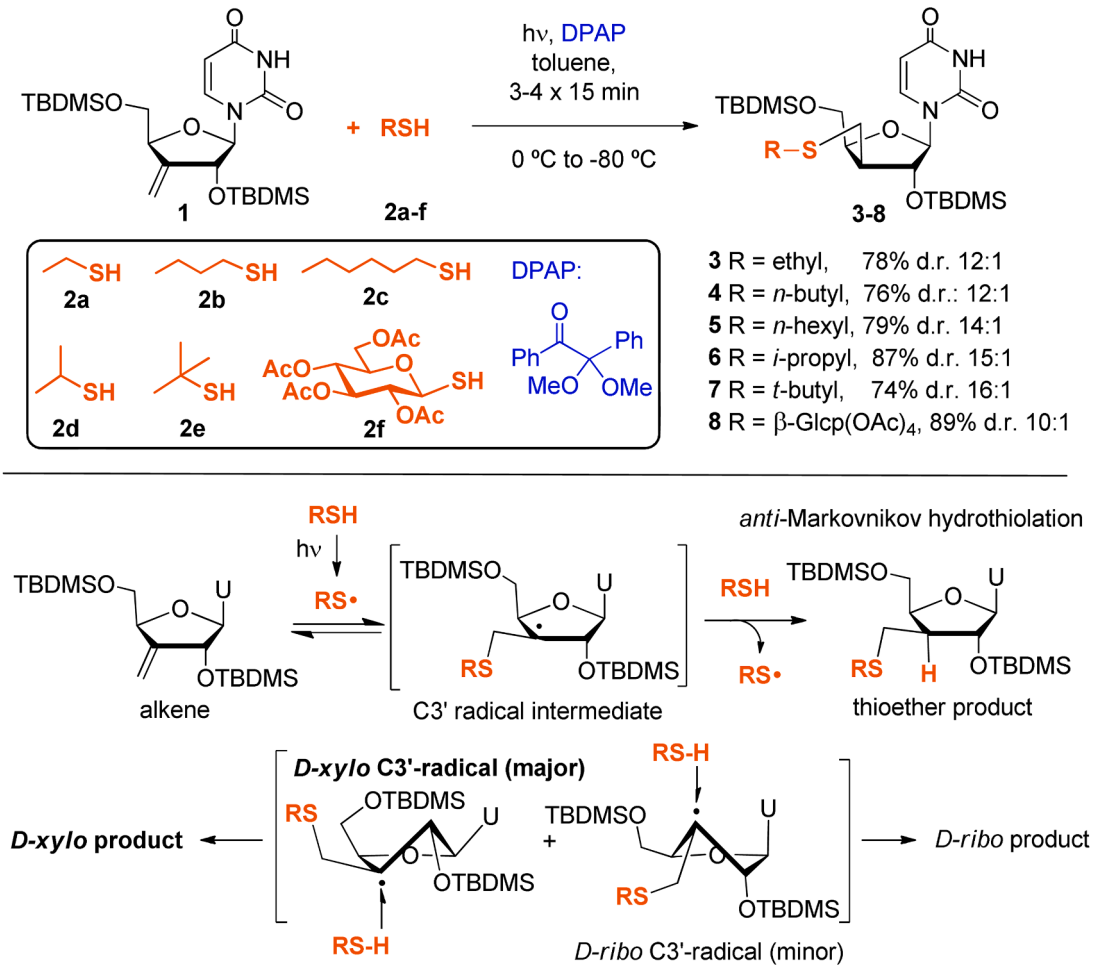

Scheme 1. Synthesis of 3′-modified nucleosides via thiol-ene coupling reaction and the mechanism of the regioselective hydrothiolation. The *xylo:ribo* diastereomeric ratio of **3**–**8** was determined by ^{1}H NMR. (TBDMS: *tert*-butyldimethylsilyl, d.r.: diastereomeric ratio).

exocyclic olefins, the reaction proceeds with moderate stereoselectivity at room temperature (Staderini et al. 2012; Borbás, 2020; Kelemen et al. 2020), but the stereoselectivity can be improved by cooling the reaction mixture. (Bege et al. 2017; Bege et al. 2019; Kelemen et al. 2019) Therefore, the reactions were carried out at −80 – 0 °C, thus obtaining the corresponding 3′-sulfanylmethyl derivatives **3**–**8** in good yields (74–89 %) and with high D-xylo-selectivity (10:1 to 16:1 xylo:ribo ratio). We hypothesize that the reaction proceeds predominantly via the more stable, fully equatorially substituted carbon-centered radical intermediate (D-xylo C3′-radical, Scheme 1), which explains the observed high degree of D-xylo-selectivity.

Next, sequential deprotection and 5′-esterification were performed on the derivatives containing various thio-substituents at the 3′-position (Scheme 2).

The primary hydroxyl group of **3**–**8** was released by selective 5′-desilylation with 50 % trifluoroacetic acid (TFA) at 0 °C, and the resulting products **10**–**14** were then esterified with butyryl chloride in pyridine at room temperature to give **15**–**20**. Finally, deprotection of the 2′-position with 90 % TFA at room temperature afforded products **21**–**26**, which have a substitution pattern similar to the antiviral drug molnupiravir. Thus, we obtained a small series of xylonucleosides, the members of which differ from each other in the 3′-substituent (six different sulfanylmethyl substituents at C3′) and the protecting group pattern (four different protecting group patterns, marked in different colors in Scheme 2).

3.2. Antiviral investigation of new derivatives

3.2.1. SARS-CoV-2 assays

The anti-SARS-CoV-2 effect of compounds **3**–**26** was first tested in Vero E6 cells (kidney epithelial cells derived from an African green monkey) and the data are summarized in Table 1.

According to the cytopathic effect-based assay, among the fully protected compounds, derivatives containing ethyl, *n*-butyl, *i*-propyl and *tert*-butyl groups at position 3′ (**3, 4, 6, 7**) showed activity against SARS-CoV-2 with EC_{50} values of 8–10 μM and selectivity indices between 1.3 and 2, while compounds **5** and **8** containing bulky *n*-hexyl and glycosyl C3’ substituents did not show any bioactivity. 5′-Desilylation reduced the cytotoxicity of most compounds, but was also detrimental to the antiviral activity, and none of the 5′-OH derivatives (**9**–**11**) showed antiviral activity at concentrations below toxic levels (highlighted in green in Table 1).

The introduction of the butyrate group at the 5′-position (highlighted in blue in Table 1) resulted in remarkable antiviral activity with EC_{50} values of 9–13 μM for *n*-butyl, *n*-hexyl, *i*-propyl and *tert*-butyl derivatives **16**–**19**, but most of them were highly cytotoxic at the active concentration. The most favorable activity profile was observed for the *tert*-butyl derivative **19**, with a selectivity index of 2.5.

Interestingly, removal of the 2′-silyl group led to complete loss of antiviral activity of the compounds. This is a surprising result, since literature data only show the benefits of lipophilic substitution at the 5′-OH. (Chamorro et al., 2001; Harmse et al., 2015; Bege et al. 2022).

The glucose peracetate-containing derivatives (**8, 14, 20, 26**) did not

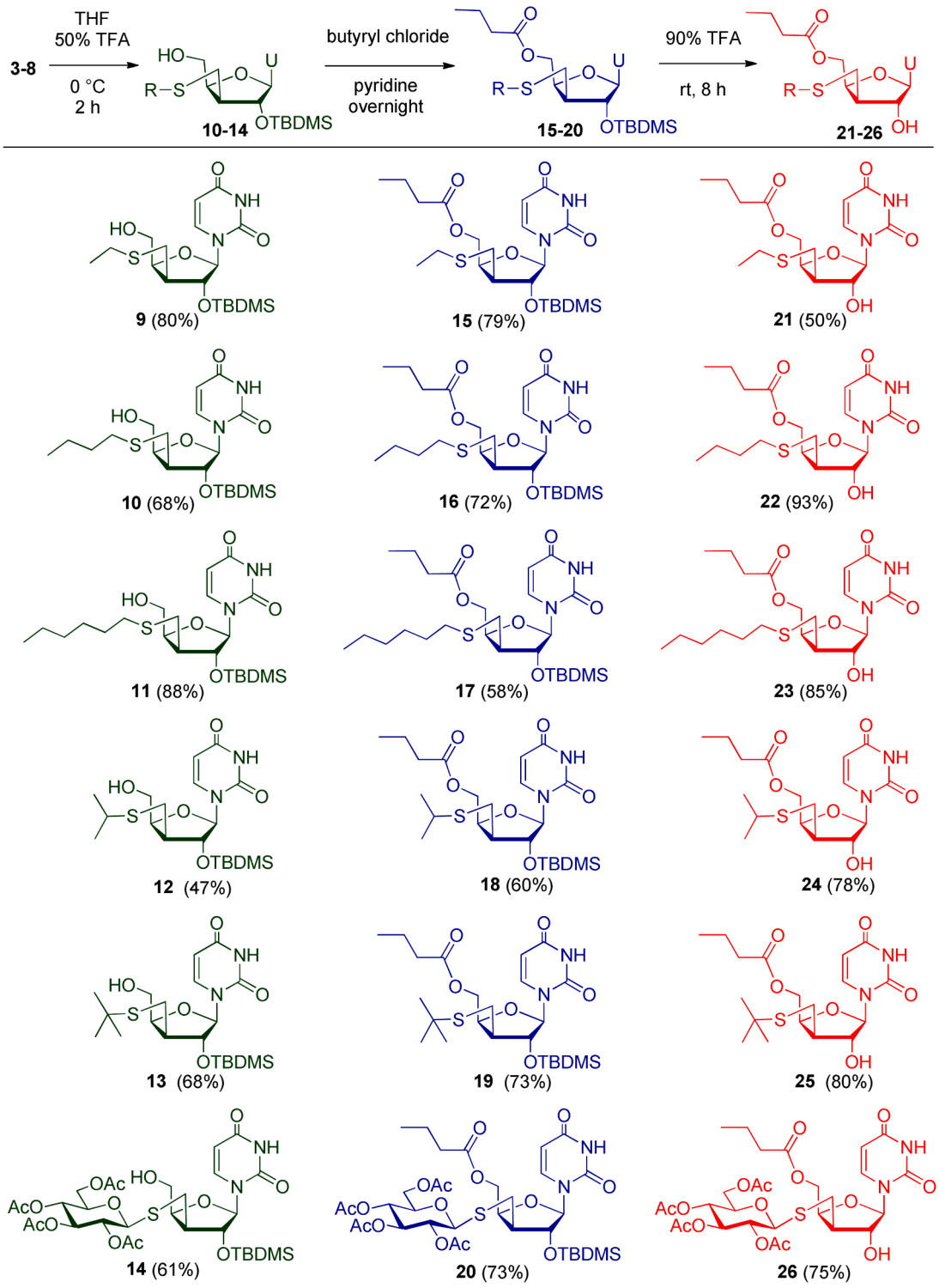

Scheme 2. Sequential deprotection and introducing the 5′-butyryl ester group. (THF: tetrahydrofuran, TFA: trifluoroacetic acid, U: uracil, TBDMS: *tert*-butyldimethylsilyl). Products with the same substitution pattern are marked with the same color (black: 2′,5′-*O*-disilyl, green: 2′-*O*-monosilyl, blue: 5′-*O*-butyryl-2′-*O*-silyl and red: 5′-*O*-butyryl).

show any bioactivity - either cytotoxicity or antiviral activity -, regardless of the substituents at the 2′ and 5′-positions.

The active compounds were also tested by immunofluorescence (IF) assay (Table 1) In the IF assay, only compounds **3, 4, 7** and **19** showed antiviral activity at subtoxic concentrations.

Four nucleosides (**3, 4, 7** and **19**), that were active in the immunofluorescence assay, were selected for further anti-SARS-CoV-2 testing in human Calu cells (Table 2). The compounds showed reduced cytotoxicity against Calu cells compared to Vero E6 cells, but their antiviral activity was also significantly reduced. Antiviral effect was only observed for the two butyl derivatives, **4** and **7**, but for the latter the antiviral EC_{50} value was the same as the cytotoxic CC_{50} value.

It is well documented that SARS-CoV-2 enters Calu cells via direct membrane fusion mediated by the host transmembrane serine protease

Table 1
Antiviral activity of the compounds against SARS-CoV-2 in Vero E6 cells.

Compound	CC_{50} ± SE[a]	EC_{50} ± SE CPE[b]	EC_{50} ± SE IF[c]	SI
3	16 ± 1.1	8.1 ± 1.1	14 ± 0.7	2/1.1
9	36 ± 2.4	>36	n.d.	-
15	31 ± 2.7	>31	n.d.	-
21	>100	>100	n.d.	-
4	13 ± 3.5	8.3 ± 0.8	8.1 ± 0.3	1.6/1.6
10	15 ± 1.7	>15	n.d.	-
16	12 ± 1.1	11 ± 1.1	>12	1.1
22	>100	>100	n.d.	-
5	>100	>100	n.d.	-
11	11 ± 1.0	>11	n.d.	-
17	12 ± 1.0	~12	>12	1
23	31 ± 7.9	>31	n.d.	-
6	13 ± 0.8	10 ± 0.9	>13	1.3
12	16 ± 1.8	>16	n.d.	-
18	14 ± 1.9	13 ± 1.5	n.d.	1.1
24	>100	>100	n.d.	-
7	16 ± 1.6	8.6 ± 0.7	14 ± 0.6	1.9/1.1
13	43 ± 3.9	>43	n.d.	-
19	~23	9.1 ± 0.8	16 ± 0.7	2.5/1.4
25	>100	>100	n.d.	-
8	>100	>100	n.d.	-
14	>100	>100	n.d.	-
20	>100	>100	n.d.	-
26	>100	>100	n.d.	-
Remdesivir	>50	2.8 ± 0.2	1.2 ± 0.03	>17.8/41.6

Concentrations are given in μM, SE standard error, SI selectivity index, n.d. not determined, a: 50 % cellular cytotoxicity concentration in Vero E6 cells det ermined by XTT assay, b: 50 % effective concentration determined by cytopathi c effect-based assay, c: 50 % effective concentration determined by immun-fluorescence assay (IF).

Table 2
Antiviral activity of selected compounds against SARS-CoV-2 in Calu cells.

Compound	CC_{50}^{a}	EC_{50}^{b}
3	32 ± 2.3	>32
4	>50	49 ± 6
7	~50	~50
19	~30	>30
Remdesivir	>50	0.6 ± 0.05

Concentrations are given in μ M, SE standard error, a: 50 % cellular cytotoxicity concentration in Calu-3 cells det ermined by XTT assay, b: 50 % effective concentration determined by cytopathic effect-based assay.

TMPRSS2 (Hoffmann et al. 2020; Tang et al. 2020). However, in Vero cells, which lack TMPRSS2, the virus enters by endocytosis (Bereczki et al. 2021; Zhao et al. 2021). The different activities of the compounds observed in the two cell lines may be due to the fact that the antiviral effect in Vero cells is, at least in part, based on the inhibition of the endosomal entry process. However, further studies are needed to elucidate the exact mechanism of the antiviral action of the compounds.

3.2.2. *Chikungunya and sindbis assays*

The antiviral activity of the new nucleoside derivatives was also evaluated against CHIKV and SINV in Vero E6 cells (Table 3). Most of the fully protected compounds (**3**–**6**) showed remarkable activity against both viruses, with EC_{50} values between 6 and 16 μM. Derivatives containing ethyl, *n*-butyl and *n*-hexyl groups as C3′-substituents (**3, 4** and **5**) were active against SINV at lower EC_{50} values than against CHIKV, while the reverse result was observed for the *i*-propyl derivative **6**. The *tert*-butyl derivative **7** showed antiviral activity against SINV at the toxic concentration. After 5′-desilylation, all 3′-alkyl derivatives (**9, 10, 11, 12** and **13**) showed antiviral activity against both viruses, although the activity of 3′-ethyl-containing **9** was significantly reduced compared to the 5′-silyl parent compound **3**. All of the 5′-OH derivatives (**9–13**) inhibited SINV with lower EC_{50} values than CHIKV. Introduction of a butyrate group into 5′-position of the derivatives containing *n*-hexyl, *i*-propyl and *tert*-butyl groups (**17, 18, 19**) resulted in remarkably high antiviral activity against both CHIKV and SINV, and these compound were slightly more active against CHIKV. Cleavage of the 2′-silyl ether group led to a complete loss of antiviral activity against both CHIKV and SINV, as was the case for SARS-CoV-2 (see above). This result confirms that lipophilic group at the 2′-position is essential for the antiviral activity of these nucleosides. Overall, the results show that the compounds with the 5′-O-butyryl-2′-O-silyl substitution pattern were most effective against CHIKV and SINV.

Table 3
Antiviral activity of the compounds against CHIKV and SINV in Vero E6 cells.

Code	CC_{50}^{a}	CHIKV $EC_{50}^{b,c}$	CHIKV SI	SINV EC_{50}^{c}	SINV SI
3	15	14.9 ± 3.4	1	9.9 ± 1.2	1.5
9	>120	57.5 ± 9.7	>2.1	32.1 ± 11.7	>3.7
15	n.d.	n.d.	-	n.d.	-
21	>120	n.a.	-	n.a.	-
4	20.1	15.3 ± 4.3	1.3	6.7 ± 0.6	3
10	29.8	13.8 ± 4.2	2.2	12.1 ± 0.9	2.5
16	n.d.	n.d.	-	n.d.	-
22	>120	n.a.	-	n.a.	-
5	>120	16.2 ± 4.7	>7.4	9.4 ± 0.5	>12.8
11	35.6	8.4 ± 0.2	4.2	5.8 ± 0.1	6.1
17	25.5	5.6 ± 1.0	4.2	5.5 ± 1.5	4.3
23	>120	n.a.	-	n.a.	-
6	31.1	8.6 ± 4.4	3.6	12.4 ± 1.0	2.5
12	66.8	26.5 ± 6.9	2.5	14.8 ± 3.8	4.5
18	44.5	8.7 ± 2.3	5.1	17.9 ± 2.4	2.5
24	>120	n.a.	-	n.a.	-
7	11.1	n.a.	-	10.9 ± 1.9	1
13	58.2	23.5 ± 2.7	2.5	10.2 ± 1.0	5.7
19	42.5	6.5 ± 0.8	6.5	14.6 ± 2.0	2.9
25	>120	n.a.	-	n.a.	-
8	>120	n.a.	-	3.4 ± 1.2	>35.3
14	>120	n.a.	-	n.a.	-
20	>120	n.a.	-	n.a.	-
26	>120	n.a.	-	n.a.	-

Concentrations are given in μM, SI selectivity index, a: 50 % cytotoxicity in Vero E6 cells det ermined by MTT assay, b: 50 % effective concentration based on MTT assay, c: ± value shows the Standard Deviation fo the EC_{50} values; n. d. not determined, n.a. not active.

Similarly to the results against SARS-CoV, glucose derivatives (**8, 14, 20** and **26**) were inactive in almost all tests. However, interestingly, the 2′,5′-disilylated glucosyl compound **8** showed highly potent anti-SINV activity.

4. Conclusion

Radical-mediated thiol-ene coupling reaction was found to be a simple and efficient method to synthesize novel nucleoside derivatives with non-natural configuration for the production of potential antiviral agents. Using this photochemical conjugation method, D-*xylo*-configured uridine analogues were prepared with high diastereoselectivity from silyl-protected 3′-exomethylene uridine with various thiols including C3-C6 alkyl thiols and per-O-acetylated 1-thioglucose. The 24-membered nucleoside set obtained by the hydrothiolation, selective 5′-desilylation, 5′-butyrylation and 2′-desilylation reaction sequence allowed the investigation of the effect of the substitution pattern on the antiviral activity of the compounds against RNA viruses.

In Vero E6 cells, 2′,5′-disilylated 3′-alkylthio compounds showed the highest antiviral effect against SARS-CoV-2, both 5′-desilylation and 2′-desilylation destroyed the activity, and surprisingly, 5′-butyryl derivatives were less active than their 5′-silylated counterparts. In human Calu cells, only the 2′,5′-disilylated 3′-*n*-butyl derivative **4** was active against SARS-CoV-2 at subtoxic concentrations. Based on the results, the antiviral effect in Vero cells may be mainly based on the inhibition of the endosomal entry process. Further studies are required to elucidate the mechanism of action observed in Calu cells.

A broader range of compounds were active against SINV and CHIKV

than against SARS-CoV-2, and the strongest activity was observed with the 5′-butyryl-2′-silyl-3′-alkylthio substitution pattern. Most of the compounds showed similar activity against the two alphaviruses; the only very interesting difference was observed with the sugar-substituted compound **8**, which was inactive against CHIKV but showed excellent antiviral activity against SINV.

Overall, the C2' and C5' substitutions play a decisive role in the antiviral activity, and surprisingly, removal of the C2' lipophilic group results in a complete loss of activity. Among the glucose-containing derivatives, the outstanding and selective anti-SINV activity of the 2′,5′-disylated conjugate **8** is noteworthy and deserves further investigation.

CRediT authorship contribution statement

Miklós Bege: Writing – original draft, Investigation. **Krisztina Leiner:** Writing – original draft, Investigation. **Miklós Lovas:** Investigation. **Réka Pető:** Investigation. **Ilona Bereczki:** Investigation. **Jan Hodek:** Investigation. **Jan Weber:** Writing – review & editing, Supervision, Funding acquisition. **Anett Kuczmog:** Writing – review & editing, Supervision, Funding acquisition. **Anikó Borbás:** Writing – review & editing, Writing – original draft, Supervision, Funding acquisition, Conceptualization.

Declaration of competing interest

There are no conflicts of interest to declare.

Acknowledgment

This research was funded by the National Research, Development and Innovation Office of Hungary (K 132870 to AB), and was supported by the University of Debrecen Scientific Research Bridging Fund (DETKA to MB) and by the University of Debrecen Program for Scientific Publication The research was also supported by the National Research, Development and Innovation Office of Hungary, RRF-2.3.1-21-2022-00010 “National Laboratory of Virology”, and Research Fund Tender program of the University of Pécs (009_2023_PTE_RK/15). The anti-SARS-CoV-2 experiments were supported by the project National Institute Virology and Bacteriology (Programme EXCELES, Project No LX22NPO5103) – funded by the European Union – Next Generation EU.

Supplementary materials

Supplementary material associated with this article can be found, in the online version, at doi:10.1016/j.ejps.2025.107107.

Data availability

Data will be made available on request.

References

Adouchief, S., Smura, T., Sane, J., Vapalahti, O., Kurkela, S., 2016. Sindbis virus as a human pathogen—epidemiology, clinical picture and pathogenesis. Rev. Med. Virol. 26, 221–241. https://doi.org/10.1002/rmv.1876.

Anderson, W.K., Coburn, R.A., Gopalsamy, A., Howe, T.J., 1990. A facile selective acylation of castanospermine. Tetrahedron Lett. 31, 169–170. https://doi.org/10.1016/S0040-4039(00)94361-2.

Bege, M., Bereczki, I., Herczeg, M., Kicsák, M., Eszenyi, D., Herczegh, P., Borbás, A., 2017. A low-temperature, photoinduced thiol-ene click reaction: a mild and efficient method for the synthesis of sugar-modified nucleosides. Org. Biomol. Chem. 15, 9226–9233. https://doi.org/10.1039/C7OB02184D.

Bege, M., Kiss, A., Kicsák, M., Bereczki, I., Baksa, V., Király, G., Szemán-Nagy, G., Szigeti, M.Zs., Herczegh, P., Borbás, A., 2019. Synthesis and cytostatic effect of 3'-deoxy-3'-C-sulfanylmethyl nucleoside derivatives with D-xylo configuration. Molecules 24, 2173–2196. https://doi.org/10.3390/molecules24112173.

Bege, M., Kiss, A., Bereczki, I., Hodek, J., Polyák, L., Szemán-Nagy, G., Naesens, L., Weber, J., Borbás, A., 2022. Synthesis and anticancer and antiviral activities of C-2'-branched arabinonucleosides. Int. J. Mol. Sci. 23, 12566–12590. https://doi.org/10.3390/ijms232012566.

Bege, M., Singh, V., Sharma, N., Debreczeni, N., Bereczki, I., Poonam, Herczegh, P., Rathi, B., Singh, S., Borbás, A., 2023. In vitro and in vivo antiplasmodial evaluation of sugar-modified nucleoside analogues. Sci. Rep. 13, 12228–12244. https://doi.org/10.1038/s41598-023-39541-4.

Bege, M., Borbás, A., 2024. The design, synthesis and mechanism of action of Paxlovid, a protease inhibitor drug combination for the treatment of COVID-19. Pharmaceutics 16, 217–234. https://doi.org/10.3390/pharmaceutics16020217.

Bereczki, I., Papp, H., Kuczmog, A., Madai, M., Nagy, V., Agócs, A., Batta, G., Milánkovits, M., Ostorházi, E., Mitrović, A., Kos, J., Zsigmond, Á., Hajdú, I., Lőrincz, Z., Bajusz, D., Keserű, G.M., Hodek, J., Weber, J., Jakab, F., Herczegh, P., Borbás, A., 2021. Natural apocarotenoids and their synthetic glycopeptide conjugates inhibit SARS-CoV-2 replication. Pharmaceuticals 14 (11), 1111. https://doi.org/10.3390/ph14111111.

Bernal, A.J., Gomes da Silva, M.M., Musungaie, D.B., Kovalchuk, E., Gonzalez, A., Delos Reyes, V., Martín-Quirós, A., Caraco, Y., Williams-Diaz, A., Brown, M.L., Du, J., Pedley, A., Assaid, C., Strizki, J., Grobler, J.A., Shamsuddin, H.H., Tipping, R., Wan, H., Paschke, A., Butterton, J.R., Johnson, M.G., De Anda, C., 2021. Molnupiravir for oral treatment of Covid-19 in nonhospitalized patients. N. Engl. J. Med. 386, 509–520. https://doi.org/10.1056/NEJMoa2116044.

Borbás, A., 2020. Photoinitiated Thiol-ene reactions of enoses: a powerful tool for stereoselective synthesis of glycomimetics with challenging glycosidic linkages. Chem. Eur. J. 26, 6090–6101. https://doi.org/10.1002/chem.201905408.

Cao, Z., Gao, W., Bao, H., Feng, H., Mei, S., Chen, P., Gao, Y., Cui, Z., Zhang, Q., Meng, X., Gui, H., Wang, W., Jiang, Y., Song, Z., Shi, Y., Sun, J., Zhang, Y., Xie, Q., Xu, Y., Ning, G., Gao, Y., Zhao, R., 2022. VV116 versus Nirmatrelvir–Ritonavir for oral treatment of Covid-19. N. Engl. J. Med. 388, 406–417. https://doi.org/10.1056/NEJMoa2208822.

Chamorro, C., Pérez-Pérez, M., Rodriguez-Barrios, F., Gago, F., de Clercq, E., Balzarini, J., San-Félix, A., Camarasa, M., 2001. Exploring the role of the 5′-position of TSAO-T. Synthesis and anti-HIV evaluation of novel TSAO-T derivatives. Antivir. Res. 50, 207–222. https://doi.org/10.1016/S0166-3542(01)00145-0.

Clarke, E.C., Nofchissey, R.A., Ye, C., Bradfute, S.B., 2021. The iminosugars celgosivir, castanospermine and UV-4 inhibit SARS-CoV-2 replication. Glycobiology 31, 378–384. https://doi.org/10.1093/glycob/cwaa091.

Cramer, N.B., Reddy, S.K., Cole, M., Hoyle, C., Bowman, C.N., 2004. Initiation and kinetics of thiol-ene photopolymerizations without photoinitiators. J. Polym. Sci. Part A. 24, 5817–5825. https://doi.org/10.1002/pola.20419.

Dondoni, A., Marra, A., 2012. Recent applications of thiol–ene coupling as a click process for glycoconjugation. Chem. Soc. Rev. 41, 573–586. https://doi.org/10.1039/C1CS15157F.

Gordon, C.J., Tchesnokov, E.P., Woolner, E., Perry, J.K., Feng, J.Y., Porter, D.P., Götte, M., 2020. Remdesivir is a direct-acting antiviral that inhibits RNA-dependent RNA polymerase from severe acute Respiratory syndrome coronavirus 2 with high potency. J. Biol.Chem. 295, 6785–6797. https://doi.org/10.1074/jbc.RA120.013679.

Harmse, L., Dahan-Farkas, N., Panayides, J., von Otterlo, W., Penny, C., 2015. Aberrant apoptotic response of colorectal cancer cells to novel nucleoside analogues. PLoS One 10, e0138607. https://doi.org/10.1371/journal.pone.0138607.

Hoffmann, M., Kleine-Weber, H., Schroeder, S., Krüger, N., Herrler, T., Erichsen, S., Schiegens, T.S., Herrler, G., Wu, N.-H., Nitsche, A., Müller, M.A., Drosten, C., Pöhlmann, S., 2020. SARS-CoV-2 cell entry depends on ACE2 and TMPRSS2 and is blocked by a clinically proven protease inhibitor. Cell 181 (2), 271–280.e8. https://doi.org/10.1016/j.cell.2020.02.052.

Hoyle, C.E., Bowman, C.N., 2010. Thiol-ene click chemistry. Angew. Chem. Int. Ed. Engl. 49, 1540–1573. https://doi.org/10.1002/anie.200903924.

Jana, M., Misra, A.K., 2013. Stereoselective synthesis of β-glycosyl thiols and their synthetic applications. J. Org. Chem. 78, 2680–2686. https://doi.org/10.1021/jo302115k.

Kelemen, V., Bege, M., Eszenyi, D., Debreczeni, N., Bényei, A., Stürzer, T., Herczegh, P., Borbás, A., 2019. Stereoselective thioconjugation by photoinduced thiol-ene coupling reactions of hexo- and pentopyranosyl D- and L-glycals at low-temperature – Reactivity and stereoselectivity study. Chem. Eur. J. 25, 14555–14571. https://doi.org/10.1002/chem.201903095.

Kelemen, V., Csávás, M., Hotzi, J., Herczeg, M., Singh, P., Rathi, B., Herczegh, P., Jain, N., Borbás, A., 2020. Photoinitiated thiol−ene reactions of various 2,3-unsaturated O-, C- S- and N-glycosides – Scope and limitations study. Chem. Asian J. 15, 876–891. https://doi.org/10.1002/asia.201901560.

Kiss, A., Baksa, V., Bege, M., Tálas, L., Borbás, A., Bereczki, I., Bánfalvi, G., Szemán-Nagy, G., 2021. MTT test and time-lapse microscopy to evaluate the antitumor potential of nucleoside analogues. Anticancer Res 41, 137–149. https://doi.org/10.21873/anticanres.14759.

Laine, M., Luukkainen, R., Toivainen, A., 2004. Sindbis viruses and other alphaviruses as cause of human arthritic disease. J. Intern. Med. 256, 457–471. https://doi.org/10.1111/j.1365-2796.2004.01413.x.

Mackman, R.L., Kalla, R.V., Babusis, D., Pitts, J., Barrett, K.T., Chun, K., Pont, V.D., Rodriguez, L., Moshiri, J., Xu, Y., Lee, M., Lee, G., Bleier, B., Nguyen, A., O'Keefe, B. M., Ambrosi, A., Cook, M., Yu, J., Dempah, K.E., Bunyan, E., Riola, N.C., Lu, X., Liu, R., Davie, A., Hsiang, T., Dearing, J., Vermillion, M., Gale Jr., M., Niedziela-Majka, A., Feng, J.Y., Hedskog, C., Bilello, J.P., Subramanian, R., Cihlar, T., 2023. Discovery of GS-5245 (Obeldesivir), an oral prodrug of nucleoside GS-441524 that exhibits antiviral efficacy in SARS-CoV-2-infected African green monkeys. J. Med. Chem. 66, 11701–11717. https://doi.org/10.1021/acs.jmedchem.3c00750.

Owen, D.R., Allerton, C.M.N., Anderson, A.S., Aschenbrenner, L., Avery, M., Berritt, S., Boras, B., Cardin, R.D., Carlo, A., Coffman, K.J., Dantonio, A., Di, L., Eng, H.,

Ferre, R., Gajiwala, K.S., Gibson, S.A., Greasley, S.E., Hurst, B.L., Kadar, E.P., Kalgutkar, A.S., Lee, J.C., Lee, J., Liu, W., Mason, S.W., Noell, S., Novak, J.J., Obach, R.S., Ogilvie, K., Patel, N.C., Pettersson, M., Rai, D.K., Reese, M.R., Sammons, M.F., Sathish, J.G., Singh, R.S.P., Steppan, C.M., Stewart, A.E., Tuttle, J. B., Updyke, L., Verhoest, P.R., Wei, L., Yang, Q., Zhu, Y., 2021. An oral SARS-CoV-2 mpro inhibitor clinical candidate for the treatment of COVID-19. Science 374, 1586–1593. https://doi.org/10.1126/science.abl4784.

Rajasekharan, S., Bonotto, R.M., Alves, L.N., Kazungu, Y., Poggianella, M., Martinez-Orellana, P., Skoko, N., Polez S., Marcello, A., 2021. Inhibitors of protein glycosylation are active against the coronavirus severe acute respiratory syndrome coronavirus sars-cov-2 viruses, 13, 808–820. https://doi.org/10.3390/v13050808.

Sanderson, T., Hisner, R., Donovan-Banfield, I., Hartman, H., Løchen, A., Peacock, T.P., Ruis, C., 2023. A molnupiravir-associated mutational signature in global SARS-CoV-2 genomes. Nature 623, 594–600. https://doi.org/10.1038/s41586-023-06649-6.

Staderini, S., Chambery, A., Marra, A., Dondoni, A., 2012. Free-radical hydrothiolation of glycals: a thiol-ene-based synthesis of S-disaccharides. Tetrahedron Lett. 53, 702–704. https://doi.org/10.1016/j.tetlet.2011.11.140.

Syed, Y.Y., 2022. Molnupiravir: first approval. Drugs 82, 455–460. https://doi.org/10.1007/s40265-022-01684-5.

Tang, T., Bidon, M., Jaimes, J.A., Whittaker, G.R., Daniel, S., 2020. Coronavirus membrane fusion mechanism offers a potential target for antiviral development. Antiviral Res. 178, 104792. https://doi.org/10.1016/j.antiviral.2020.104792.

Thakur, S., Sasi, S., Pillai, S.G., Nag, A., Shukla, D., Singhal, R., Phalke, S., Velu, G.S.K., 2022. SARS-CoV-2 mutations and their impact on diagnostics, therapeutics and vaccines. Front. Med. (Lausanne). 22, 815389. https://doi.org/10.3389/fmed.2022.815389.

Vu, D.M., Jungkind, D., LaBeaud, A.D., 2017. Chikungunya Virus. Clin. Lab. Med. 37, 371–382. https://doi.org/10.1016/j.cll.2017.01.008.

Weaver, S.C., Lecuit, M., 2015. Chikungunya Virus and the global spread of a mosquito-borne disease. N. Engl. J. Med. 372, 1231–1239. https://doi.org/10.1056/NEJMra1406035.

Weaver, S.C., Charlier, C., Vasilakis, N., Lecuit, M., 2018. Zika, Chikungunya, and other emerging vector-borne viral diseases. Annu. Rev. Med. 69, 395–408. https://doi.org/10.1146/annurev-med-050715-105122.

Zhao, M.-M., Yang, W.-L., Yang, F.-Y., Zhang, L., Huang, W.-J., Hou, W., Fan, C.-F., Jin, R.-H., Feng, Y.-M., Wang, Y.-C., Yang, J.-K., 2021. Cathepsin L plays a key role in SARS-CoV-2 infection in humans and humanized mice and is a promising target for new drug development. Signal Transduct. Target. Ther. 6 (1), 134. https://doi.org/10.1038/s41392-021-00558-8.